THE UNIVERSITY OF ALBERTA

A Study of the Performance of a Solar Air Heating System

by

Philip Tak Ning Fung

A THESIS

SUBMITTED TO THE FACULTY OF GRADUATE STUDIES AND RESEARCH

IN PARTIAL FULFILMENT OF THE REQUIREMENTS FOR THE DEGREE

OF Master of Science

Department of Mechanical Engineering

EDMONTON, ALBERTA

Spring 1983

Abstract

The performance of the active air solar heating system installed in Module 6 of the Alberta Home Heating Research Facility was evaluated for the September 1981 to March 1982 heating season. The operating characteristics and energy flows for the system were examined and the performance parameters calculated.

The solar contribution assessed by direct and indirect methods ranged from 11.3 to 17.8 %. The indirect methods yielded values that were close to the measured solar contribution.

The solar collector was constructed from six commercial collectors and its performance was calculated on an instantaneous, hourly, daily and monthly basis. For this solar collector, the $Fr(\tau\alpha)\epsilon$ ranged from 0.53 to 0.56, and all values were higher than the performance test value of 0.5. The collector heat loss coefficient FrU^L ranged from 1.43 to 2.61 $W/m^2-^{\circ}C$. The monthly value FrU^L of 2.61 $W/m^2-^{\circ}C$ is closer to the manufacturer's performance test value of 2.9 $W/m^2-^{\circ}C$ and is probably more representative of the collector heat losses.

Energy flows for the components of the system were evaluated. The 2 m^3 rock bed storage bin was fully charged during periods in September 1981 when heating requirements were low. About 23.6 % of the 3525.3 MJ of total energy stored was transferred from the bin.

Acknowledgements

The author wishes to express his sincere appreciation to the persons who have helped to bring this study to completion. In particular, thanks are due to Professor G.W. Sadler, who, as Supervisor of the Thesis Committee, offered valuable suggestions and constructive criticism throughout. The author also wishes to thank the other members of the Committee, Dr. J.D. Dale and Dr. A.M. Robinson for their ideas and assistance.

The author wishes to thank Mr. M.Y. Ackerman for his assistance with data acquisition, and for his helpful suggestions regarding the treatment of the data.

Table of Contents

List Of Tables

List Of Figures

Nomenclature

<u>Notation</u>

Ac   Transparent frontal area for a flat-plate collector, [m²]

Ag   Gross collector area, [m²]

COL   Operation time for heat-collection mode, [min]

Cp   Specific heat of the transfer fluid, air, [J/kg-°C]

EH   Operation time for electric heating mode, [min]

DTCcol   Hourly sum of temperature difference across collectors in heat-collection mode, [°C-s]

DTChfc   Hourly sum of temperature difference across collectors in heat-from-collector mode, [°C-s]

DTScol   Hourly sum of temperature difference across storage bin during heat-collection mode, [°C-s]

DTSeh   Hourly sum temperature difference across storage bin during electrical heating mode, [°C-s]

DTShfs   Hourly sum of temperature difference across storage bin in heat-from-storage mode, [°C-s]

dTC   Instantaneous temperature difference measured across collectors, Tfe-Tfi, [°C]

dTS   Instantaneous temperature difference measured across storage bin, Tst-Tsb, [°C]

f   Monthly solar contribution assessed by F-chart prediction, dimensionless

Fua   Power correction factor, dimensionless

Fr   Solar collector heat removal factor, dimensionless

HFC   Operation time for heat-from-collector mode, [min]

HFS	Operation time for heat-from-storage mode, [min]
Ht	Total solar radiation on the tilted surface, [W/m²]
I	Total no. of hours corresponding to each operation mode in a day, [Hr]
K	Total no. of hours corresponding to each operation mode in a month, [Hr]
$\bar{m}$	Mass flow rate of air, [kg/s]
Qas	Actual monthly solar energy supplied from the thermal system to space heating, [J]
Qbhl	Hourly energy losses from the module through conduction, [W]
Qccol	Hourly solar energy gained from collector during heat-collection mode, [J]
Qchfc	Hourly solar energy gained from collector during heat-from-collector mode, [J]
Qeh	Hourly energy supplied during electric heating mode, [J]
Qeh5	Hourly electric power usage in module 5, [W]
Qeh6	Hourly electric power usage in module 6, [W]
Qht	Hourly total energy supplied or required for space heating, [J]
Qmeh	Monthly electric energy usage, [J]
Qmsun	Monthly solar energy gained from collector, [J]
Qmas	Monthly actual solar energy supplied from the thermal system to space heating, [J]
Qmsa	Monthly total active solar energy required for space heating, [W]

Qscol   Hourly energy entering the storage bin from collector, [J]

Qseh   Hourly energy supplied from storage bin for space heating during electric heating mode, [J]

Qshfs   Hourly energy supplied from storage bin for space heating during heat-from-storage mode, [J]

Qsloss   Hourly energy losses from storage bin by air leakage or conduction through bin walls, [J]

Qsto   Hourly energy stored or accumlated in the storage bin, [J]

Qsysl   Monthly energy transfers or losses from the thermal system, [J]

Ta   Ambient air temperature, [°C]

Tfi   Temperature of transfer fluid entering the collector, [°C]

Tfe   Temperature of transfer fluid leaving the collector, [°C]

Tp   Average temperature of the collector absorbing surface, [°C]

Tr   Room temperature, [°C]

Tsb   Temperature of transfer fluid at the bottom of storage bin, [°C]

Tst   Temperature of transfer fluid at the top of storage bin, [°C]

UA   Building heat loss coefficient (UA Factor), [W/°C]

ξd Daily collector efficiency, dimensionless

ξh Hourly collector efficiency, dimensionless

ξi	Steady state instantaneous collector efficiency, dimensionless
ξm	Monthly collector efficiency, dimensionless
Ls	Monthly fraction of energy transfers or losses from the storage bin, dimensionless
Lsd	Monthly fraction of energy transfers or losses from the storage bin and the duct section, dimensionless
Lsys	Monthly fraction of energy transfers or losses from the thermal system, dimensionless
ηbhl	Monthly solar contribution assessed by building heat loss method, dimensionless
ηeh	Monthly solar contribution assessed by power records method, dimensionless
ηr	Monthly solar contribution assessed by solar required method, dimensionless
ηs	Monthly solar contribution assessed by solar supply method, dimensionless
$P\gamma$	Monthly power ratio for module 5 and 6, dimensionless
$P\gamma a$	Monthly actual power ratio for module 5 and 6, dimensionless
α	Absorptance of the collector absorber surface for solar radiation, dimensionless
τ	Transmittance of the solar collector cover plate, dimensionless

$(\tau\alpha)_n$ Effective transmittance-absorptance product at
         normal incidence, dimensionless

$(\tau\alpha)_\epsilon$ Effective transmittance-absorptance product,
         dimensionless

U_L Solar collector heat transfer loss coefficient,
         $[W/m^2-{}^\circ C]$

ρ Air Density, $[kg/m^3]$

1. Introduction

The production rate of petroleum liquid for the North American continent appears to have reached a maximum and may now be decreasing. Foreign sources of petroleum liquid are the major supplementary sources of energy and these also may be exhausted in the foreseeable future. In order to ensure a continuous supply of energy, the adoption of conservation measures and the developing and deploying other energy sources are necessary. As a consequence, a number of researchers and practicing engineers changed their focus from non-renewable fossil fuel technologies to renewable power sources or technologies for reducing the consumption of fossil fuels. Many people in this field agree that solar energy is one of the most significant of the renewable energy sources. The potential of solar energy assessed by the U.S. National Science Foundation in the testimony before the U.S. Senate Interior Committee in 1972 was that solar energy is the most promising of the unconventional energy sources potentially capable of meeting a significant portion of the future energy needs[28].

In recent years, residential energy consumption has become a very topical subject studied by many researchers. All of them tried to reduce auxiliary space heating requirements by a number of solar heating schemes, both active and passive. The result was many demonstration houses that modified the present house design in Canada and the United States.

The Alberta Home Heating Research Facility, which was constructed in the summer of 1979, is an experimential research facility consisting of six 6.7 x 7.3 x 5.0 m single story modules with full basements. These modules are located on the University of Alberta Farm in a single East-West row and are designed to test domestic heating strategies in a northern climate. The modules are unoccupied. Two of the modules, module 5 and 6 were constructed firstly to compare the performance of two identical constructions under in situ conditions, and secondly to assess the operating characteristics of two active solar systems with different working fluids operating under the same meteorological conditions. However, because of budgetary constraints, only the active air heating system was installed. Details of this facility are presented in Chapter 2.

Since the performance of a solar air heating system is a complex function of weather, system design, and collector area in relation to the load, a meaningful rating system also becomes very complex. A number of researchers such as Lunde[8],[9]; Klein, Beckman, Duffie[11]; Löf, Shaw, Oank[17]; Hill[23]; Gupta,Garg[14]; Hollands, Chineck, Chanarashekar[42]; and Close[6] proposed many methods of studying the monthly and annual performance of solar air heating systems. All of them emphasised the thermal performance of the collector and some considered both the performance of collector and storage bin.

Also, interactive computer programs for solar heating and cooling design have been developed by many designers. Two computer programs are in widespread use in connection with modeling or sizing of solar air heating system. The program called TRNSYS, which is for simulating the hour by hour dynamic thermal behavior of active solar heating and cooling systems, was developed by Klein, et al.[31]. Another program called F-chart, which is for simulating the long-term performance of solar heating or cooling system, was developed by Beckman, Duffie and Klein[30].

Although several methods for rating of solar heating systems have been proposed, it seems that many of them do not fully meet the requirements of technical and non-technical users of solar heating system. For the technical users, the solar collector performance, the storage bin performance and the solar space heating contribution are the main parameters to assess the performance of a solar heating system. The collector performance represents the heat delivery capability of the solar collector and is usually obtained from a graph of collector efficiency plotted as a function of the difference in inlet and ambient temperature divided by solar radiation on the collector tilted surface, $(Tfi-Ta)/Ht$. This collector efficiency curve can be applied to computer programs to assess the solar contribution. For the non-technical user, the solar heating contribution is the main parameter to assess the thermal performance of a solar heating system.

Several national standards for rating solar collector have been developed, including those of the Air Conditioning and Refrigeration Institute[3], (ARI), the Solar Energy Industries Association[4], (SEIA), and the Solar Energy Research and Education Foundiation [5], (SEREF). All of these rating methods are based on the same collector testing method. This method, which was developed by the National Bureau of Standards and further refined by the American Society of Heating, Refrigerating, and Air Conditioning Engineers is now known as the ASHRAE 93-77 collector testing method[1]. However, the testing is done under cloudless sky conditions with uniform solar radiation and may not be representative of the dynamic behaviour of solar collectors in the real environment.

The present study is mainly concerned with the performance of the active air heating system during the September 1981 to March 1982 heating season. The operating characteristics and energy flows for the system are examined and the performance parameters are calculated. Methods of assessing the solar contribution for the technical and non-technical solar heating users are presented in Chapter 3. The collector performance examined on an instantaneous, hourly, daily, and monthly basis is presented in Chapter 4. The storage bin characteristics are also included in this chapter.

In addition, the assessment of the system performance should include the effect of energy losses. Losses from the

storage bin and ducts go into the module interior and usually contribute to the heating requirement during the heating season. These are called the useful energy losses. However, the same losses can also cause module overheating during the summer and add to the cooling load. Therefore the present work also estimates the energy losses transferred from the bin walls and ducts to the space. These losses are presented in Chapter 4.

In Chapter 5, the results of solar heating contribution assessed by different methods, collector and storage bin performance, dynamic behavior of storage bin and energy losses are discussed. This is followed by the conclusions drawn from this study.

2. The Solar Module

2.1 Introduction

The thermal performance of the solar air heating system is estimated or predicted from the gathered data for module 5 and 6 on a continuous basis. The construction details for modules 5 and 6, the components of the solar air heating system, the system operation modes, data measurement and the data acquisition system are presented in this chapter.

2.2 Construction Details For Module 5 And Module 6

Modules 5 and 6 of the test facility are idential in contruction except for the ceiling insulation level of module 6 which is about 63 percent higher than that of module 5. The main floor plan for each module and wall section are shown in Figure 2.1 and Figure 2.2 , and the design details are given in Table 2.1 . The construction of the modules represented pre 1970 construction standards for housing in Alberta. By using identical modules, module 5 could be used as a control module to study the performance of a solar heating system installed in module 6.

2.3 The Solar Heating System

A schematic diagram of the solar air heating system installed in module 6 for space heating during the summer of 1980 is shown in Figure 2.3 . The principal components of the solar air-heating system are the collector, the heat
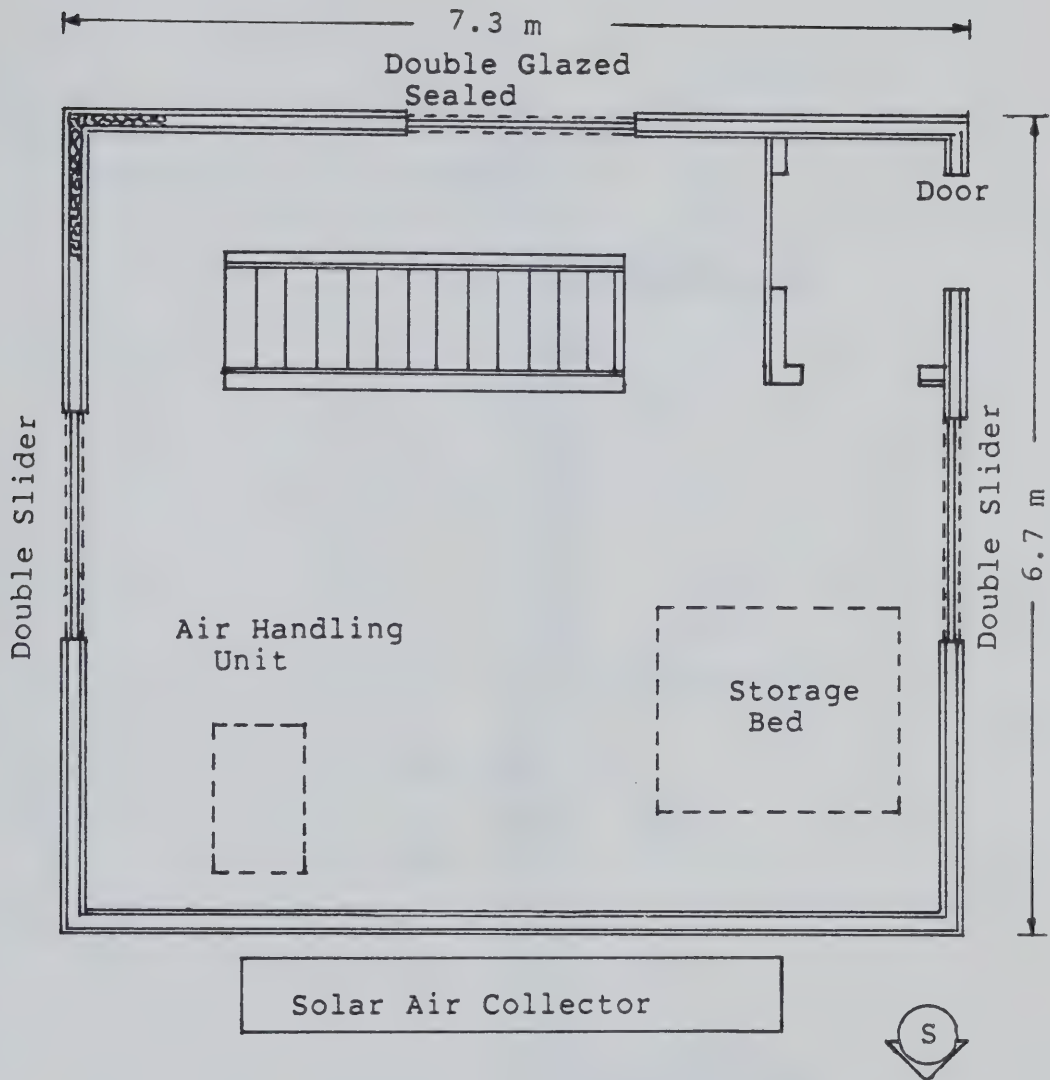
Figure 2.1 Main Floor Plan
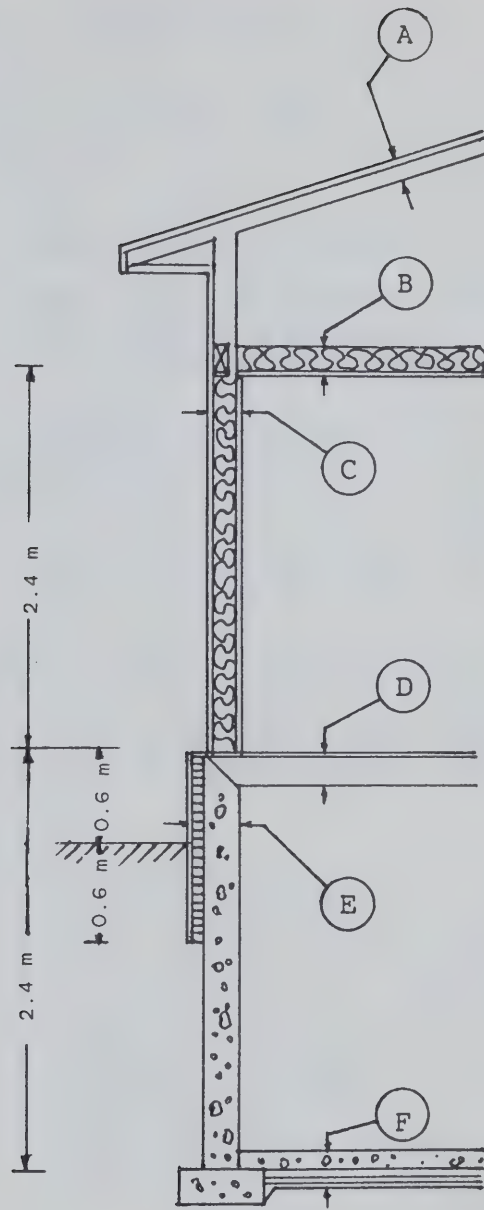
Figure 2.2 Wall Section
        A, B, C, D, E, F illustrated in Table 2.1

Table 2.1 Design Details Of The Module 5 And 6

                    RSI - (sq-m-K/Watt)

Floor Area(exterior) : 6.7m x 7.3m
           (interior) : 6.5m x 7.1m

Main Floor Wall Height : 2.4m

Basement Height : 2.4m, 1.8m below grade

Roof   (A): CMHC approved trusses with 0.6m-15cm stub
                : 210# asphalt shingles
                : 1.0cm plywood Ext,GD sheathing

Ceiling   (B): standard truss with 0.6m bobtail rafters
                     0.6m on center
                : fiberglass insulation (RSI 5.46) module 6
                                        (RSI 2.11) module 5
                : 100 micrometre (4 mil) poly vapour barrier
                : 1.3cm drywall painted

Wall   : 1.0cm Prestain Rough Tex Plywood
Construction (C): 8.9cm fiberglass insulation (RSI 1.76)
                : 5.1cm x 10.2cm studs, 40.6cm on center
                : 100 micrometre (4 mil) ploy vapour barrier
                : 1.3cm drywall painted

Wall Area / Floor Area : 1.39

Main Floor   (D): 1.6cm fir plywood
                : 5.1cm x 20.3cm studs, 40.6cm on center

Basement Wall(E): 1.3cm preservative treated plywood
                  to 0.6m below grade
                : 5.1cm rigid insulation (RSI 1.76)
                  to 0.6m below grade
                : 20.3cm concrete wall
       Floor(F): 10.2cm concrete slab on 150 micrometre
                  (6 mil) poly vapour barrier

Windows North   : 90cm x 193cm double glazed sealed
        South   : None
        East   : 102cm x 193cm double slider
        West   : 102cm x 193cm double slider

Window Area / Floor Area : 11.9 %

Door   : 91.4cm x 203.2cm insulated metal

Electric Duct   : 7.5 kW
Heater Capacity
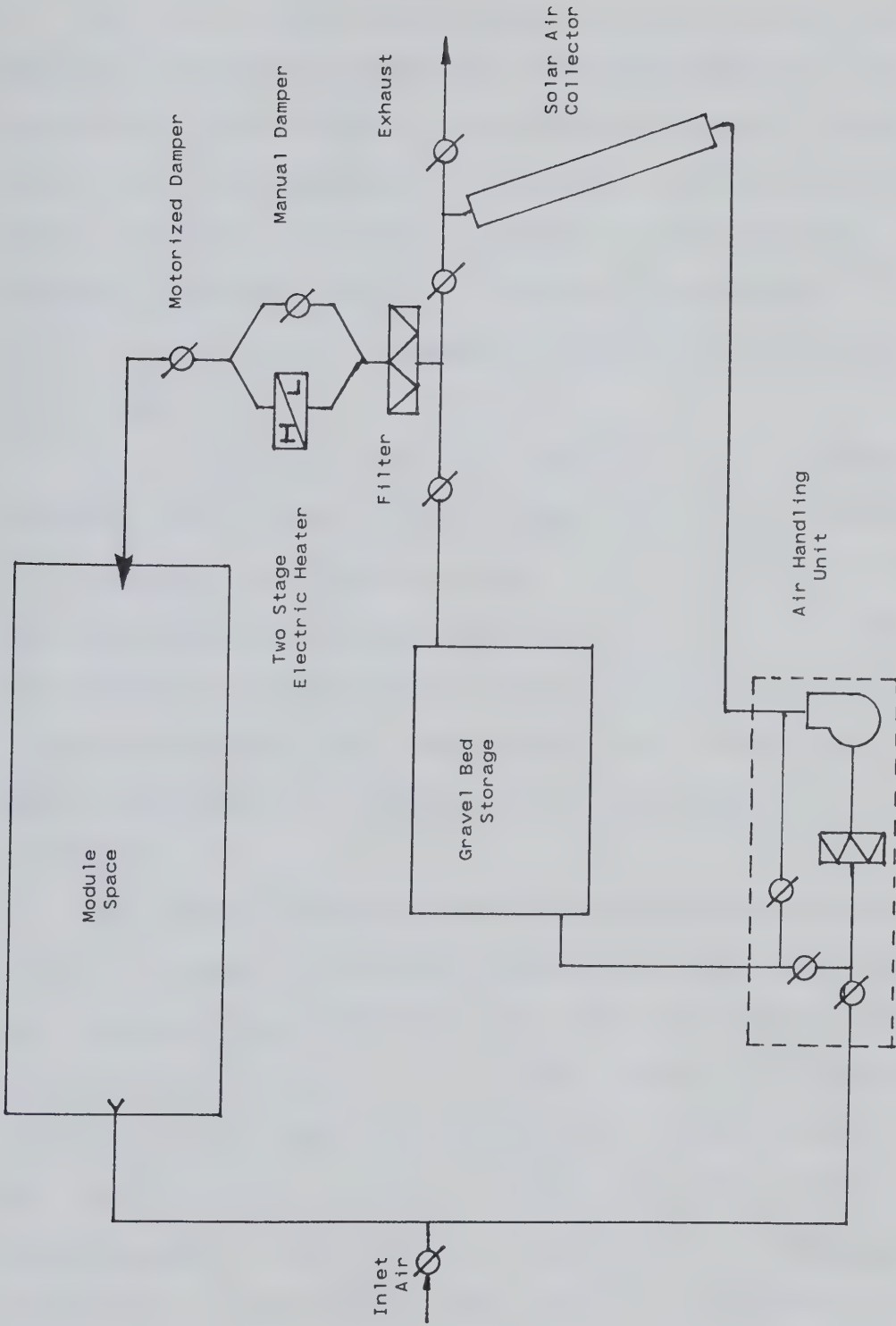
Figure 2.3 Schematic Solar Air System

storage facility, the air handling system and control
system.

A 11.1 m² south facing solar collector tilted at 70
degrees to the horizontal was installed adjacent to the
south wall. The collector was assembled using 6 Solaron
series 2000 flat plate air collectors by connecting two in
series and mounting three of these units in parallel. This
assembly provided a total air heating path length of about
3.5 m. The collector is double glazed and has an enamelled
steel absorber.

A 2 m³ washed gravel heat storage bin is located in the
basement. The bin is of wood frame construction with 89 mm
of fiberglass insulation and the interior surface of the bin
has 50.8 mm of styrofoam insulation applied to it. The rock
bed rests on the basement floor with 50.8 mm of styrofoam
insulation between the lower plenum and the basement floor.
Typical parameters of collector and storage bin are shown in
Table 2.2 .

The other components are an air handling unit, a
control system with sensors and relays, motorized dampers
for properly directing the flow, and a two stage electric
furnace back up heater. An internal by-pass with appropriate
dampers in the handling unit permits a single blower to move
air in all of the necessary system operation modes. The
by-pass makes it possible for the blower to supply solar
heated air to the storage bin and also to withdraw hot air
(in the opposite direction) from the same end of the storage

Table 2.2 Solar Air-Heatering System Parameters

Collector Orientation	South Facing
Collector Tilted From Horizontal	70 degrees
Collector Gross Area	11.1 m²
Collector Net Area	9.642 m²
Storage Volume And Materials	2.0 m³ Washed gravel
Specific Heat Of Rock	0.88 kJ/kg°C
Storage Capacity Per Area Of Collector	545.6 kJ/m²-°C
Air Flow Rate	0.122 m³/s 0.011 m³/s-m²
Electric Furance Capacity	7.5 kW

bed.

2.4 System Operation Modes

The control system is designed to operate in five basically distinct modes of operation. A schematic of the air-flow loop for each mode is shown in Figure 2.4 .

(1) Heat From Collectors

If space heating is required and the air temperature at collector outlet is 9 °C above the room temperature, then air is circulated through the collector, by-passes the storage unit and is sent directly to the space. If the collector outlet air temperature is less than 18 °C above room temperature, the first stage electric heater is used to keep the room temperature above 18 °C.

(2) Heat Collection(Storage)

If no space heating is required and the air temperature at collector outlet is 9 °C above the storage temperature, air is circulated from collectors to the storage unit and returned to the collector.

(3) Heat From Storage

If space heating is required and no energy is available from the collector, air is circulated in the opposite direction through the storage unit and sent directly to the room. If the air temperature off the storage unit is less
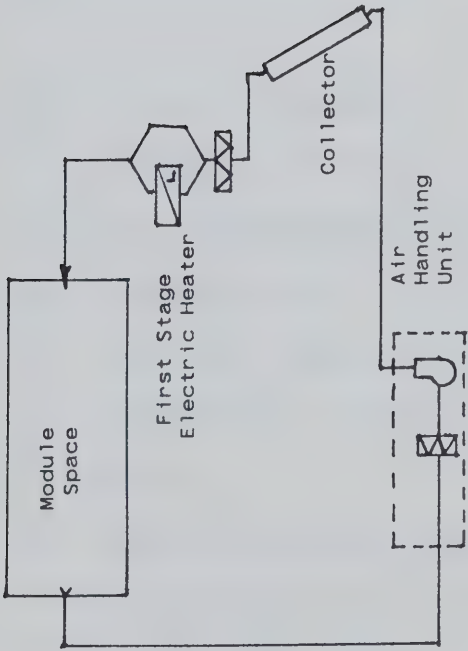
(1) Heat From Collector
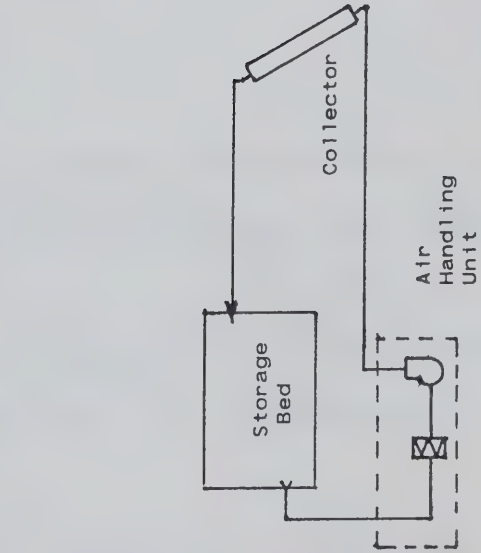
(2) Heat Storage
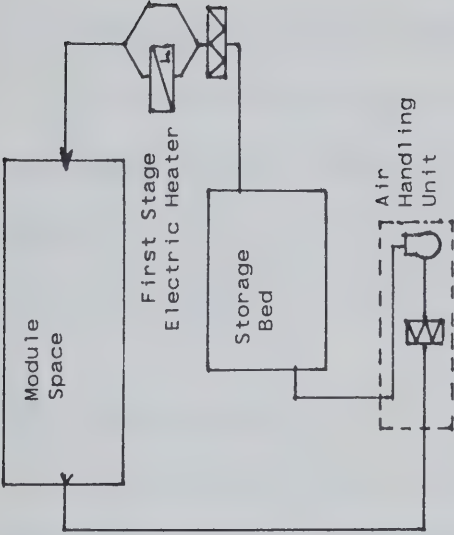
(3) Heat From Storage
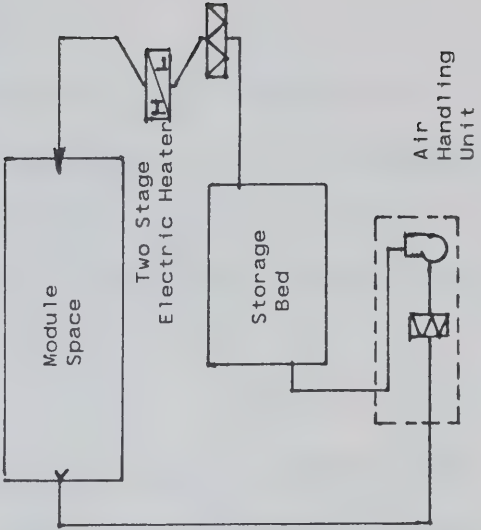
(4) Stage Heating

Figure 2.4 Schematic Air Flow Loop For Each Mode

than 18 °C above the room temperature, the first stage
electric heater is used.

(4) Stage(Electrical) Heating

If space heating is required, but no energy is
available from either the collectors or the storage unit,
then both the first and second stage heaters are in
operation with air circulating through the storage unit.

(5) System Purge

If the collector temperature is above the maximum
allowable limit, outside air can be circulated through the
collector and exhausted to the ambient in order to prevent
the collector overheating.

2.5 Meteorological And Measured Data

2.5.1 Data Measurement

Figure 2.5 shows the locations of temperature and solar
radiation measurements for module 6. The data measurements
can be summarized as:

1. Electric usage is measured on an hourly basis by adding
    an optical counter to the disk of a standard power
    meter.

2. Temperatures are measured using copper-constantan
    thermocouples with cold junction compensation provided
    by the data logger.
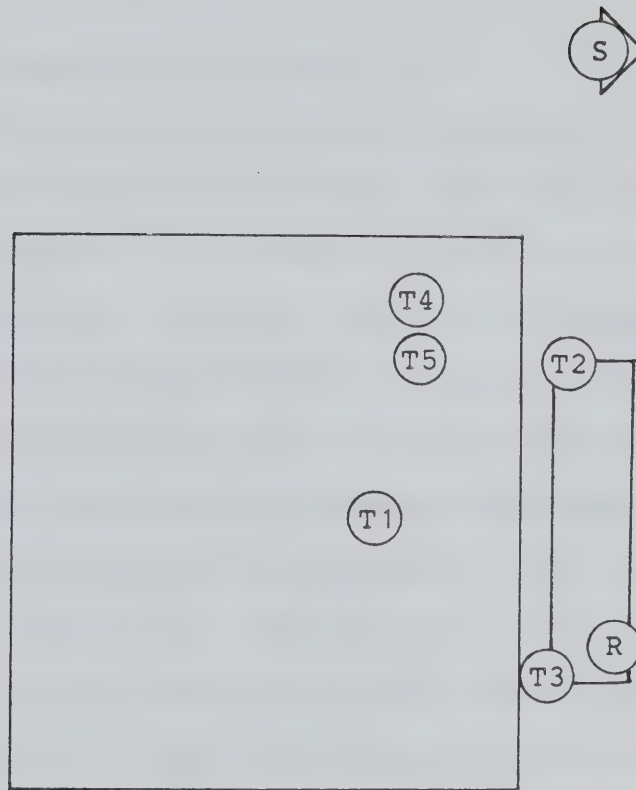
T1 - Room Temperature
T2 - Collector Inlet Air Temperature
T3 - Collector Outlet Air Temperature
T4 - Air Temperature At The Top Of The Bin
T5 - Air Temperature At The Bottom Of The Bin
R - Total Radiation On Collector Surface

Figure 2.5 Measurement Locations In Module 6

3. Horizontal surface radiation, diffuse radiation, and the
    solar radiation on the tilted collector surface are
    measured by Eppley pyranometers.

2.5.2 Data Acquisition System

Control of the data logging operation was accomplished
using an Analog Device MACSYM II computer controlled data
acquisition system. The modes of operation for the collector
system, the solar radiation, the electric usage, the air
temperature for the collectors, storage bin and space were
monitored by the data logger every two minutes. At the end
of each hour, the logger provides totals and averages, and
after a 24 hour period has passed, the data was transferred
to magnetic tape in the University computer system. Then the
memory was cleared and the sequence begins again.

In addition, when solar energy collection occurs, a
printed record of the 2 minute interval measurement was made
to facilitate detailed analysis of the behavior of system
components.

3. Methods For Assessing Solar Contribution

3.1 Introduction

The solar contribution is a main parameter for the design and installation of a thermal system. Direct methods and indirect methods can be used to assess the solar contribution. The direct methods compute the solar contribution based on the measured solar records. The two methods are:

1. The solar supply method: the solar contribution based on the energy collected by the collector.
2. The solar required method: the solar contribution based on the measured energy supplied by the system components.

For the indirect methods, 3 approaches have been taken:

1. The building heat loss method: the solar contribution based on the calculated energy loss and the non-solar internal energy gains.
2. The power records method: the solar contribution based on the power consumption of the test module and a control module.
3. The F-chart method: a computer program developed at the University of Wisconsin for theoretical predictions of the long-term solar contribution.

All these methods will be discussed in this chapter.

3.2 Direct Methods

These methods compute the solar contribution from detailed measurements of the solar energy gained from the solar system. The data required for assessing the solar contribution includes the temperature difference across collector and storage bin during each of the operating modes, and electical power usage for the module. The two minute interval records of the electrical power usage and temperature difference data were summed at the end of each hour, and hourly values were used in the analysis.

The hourly average temperature difference across collectors or storage bin can be computed by dividing the cummulative hourly temperature difference by the number of temperature readings recorded in each hour. The number of temperature readings recorded in each hour can be determined by dividing the number of minutes in each corresponding mode by two. The hourly sum of the temperature difference can be computed by mutiplying the hourly average temperature by the number of minutes recorded in each corresponding mode. The unit of time in minutes is then converted to seconds to give the hourly temperature differences in degree celcius second.

The hourly sum of temperature difference across the collector in each operation mode with the unit in degree celcius second is given by:

$$DTCcol = (\sum_{i}^{COL} dTC) \times 2 \times 60 \qquad (3.1)$$

$$DTChfc = (\sum_{i}^{HFC} dTC) \times 2 \times 60 \qquad (3.2)$$

And the hourly sum of temperature difference across storage bin for each operation mode is given by:

$$DTSeh = (\sum_{i}^{EH} dTS) \times 2 \times 60 \qquad (3.3)$$

$$DTShfs = (\sum_{i}^{HFS} dTS) \times 2 \times 60 \qquad (3.4)$$

$$DTScol = (\sum_{i}^{COL} dTS) \times 2 \times 60 \qquad (3.5)$$

Where

EH = no. of minutes in the electric heating mode
HFS = no. of minutes in the heat-from-storage mode
HFC = no. of minutes in the heat-from-collector mode
COL = no. of minutes in the heat-collection(storage) mode
dTC = instantaneous air temperature difference measured
      across collector, Tfe-Tfi, [°C]
dTS = instantaneous air temperature difference measured
      across storage bin, Tst-Tsb, [°C]

3.2.1 Solar Contribution Using Solar Supply Method

The energy collected by the solar collector is the maximum solar energy availiable to Module 6. The collector operates into 2 modes: the heat-from-collector mode in which the collected energy is sent directly to space heating, and the heat-collection(storage) mode with the collected energy sent directly to the storage unit. The maximum energy supplied is the sum of the energy delivered from the solar collector in each operation mode and the electrical energy supplied. The hourly collected energy can be estimated by multiplying the hourly sum of temperature difference across collectors by the product of the mass flow rate and fluid heat capacity. The maximum hourly energy supplied to space heating can be estimated by:

$$Qhsun = Qchfc + Qccol \qquad\qquad (3.6)$$

$$Qht \ \ = Qhsun + Qeh \qquad\qquad (3.7)$$

Where

Qhsun = hourly solar energy gained from the collector, [J]
Qchfc = hourly energy gained from collector
        for space heating(heat-from-collector mode),
        $\bar{m}Cp(DTChfc)$, [J]
Qccol = hourly energy gained from collector for storage
        (heat-collection mode), $\bar{m}Cp(DTCcol)$, [J]
Qeh   = hourly energy supplied from electric (stage)
        heating mode, [J]
Qht   = hourly total energy supplied for space heating, [J]

The cumulative monthly solar energy supplied for space heating (Qmsun) can be determined from:

$$Qmsun = \sum_{k}^{K} Qchfc + \sum_{k}^{K} Qccol \qquad (3.8)$$

The cumulative monthly total electric energy usage (Qmeh) is:

$$Qmeh = \sum_{k}^{K} Qeh \qquad (3.9)$$

Therefore the maximum solar contribution supplied to space heating can be estimated as:

$$\eta s = \frac{Qmsun}{Qmsun + Qmeh} \qquad (3.10)$$

3.2.2 Solar Contribution Using Solar Required Method

Using this method, the solar contribution can be assessed by computing the total energy required for space heating by an energy balance for the module. Total energy required for space heating can be estimated by summing the collected energy from the collector that is immediately used for space heating, the energy supplied from storage bin, the energy supplied from storage bin during electrical heating and the electrical energy usage. Thus, the hourly total

energy required for space heating can be written as:

$$Qht = Qchfc + Qshfs + Qseh + Qeh \qquad (3.11)$$

Where

Qht = hourly total energy required for space heating, [J]
$Qshfs$= hourly energy supplied from storage bin for space
        heating (heat-from-storage mode), $\bar{m}Cp(DTShfs)$, [J]
$Qseh$ = hourly energy supplied from storage bin with
        auxiliary heater operating (heat from storage bin
        during electric heating mode), $\bar{m}Cp(DTSeh)$, [J]

$Qchfc$ and Qeh are the same as declared in Equations 3.6
        and 3.7

The cumulative monthly total energy required for space
heating can be determined by:

$$Qmt = \sum_{k}^{K} Qht \qquad (3.12)$$

By combining Equations 3.9 and 3.12 , the monthly solar
contribution required for space heating can be assessed as
follows:

$$\eta r = 1 - \frac{Qmeh}{Qmt} \qquad (3.13)$$

3.3 Indirect Methods

3.3.1 Solar Contribution Using Building Heat Loss Method

In the process of transferring solar energy from the collectors, significant energy losses may occur for active solar systems. As an alternative to using detailed measurements to determine the energy losses of an active air solar system, a method studied by Taylor[16] called the building heat loss method can be modified to evaluate the solar space heating contribution of the solar system. This method, which defines the building(module) as the analysis control volume, can be used to assess the solar contribution with a minimum of instrumentation and data acquisition.

The overall solar contribution for space heating can be computed as follows:

$$
\begin{array}{ccccc}
\text{Overall} & & \text{Building} & & \text{Non-solar} \\
\text{solar} & = & \text{heat} & - & \text{internal} \\
\text{contribution} & & \text{loss} & & \text{energy gains}
\end{array} \qquad (3.14)
$$

The overall solar contribution is the sum of the net passive energy gains (Qsp) and the solar energy supplied to the building interior by the active system (Qsa). Direct passive windows gains of small magnitude can be estimated by using measured radiation data. The estimated passive gain is substracted from the computed overall solar contribution to obtain the active system contribution.

Non-solar internal energy gain is the electrical power supplied to the module which includes:

1. The power for electrical heater
2. The power for lighting, and
3. The power for the heating system fan.

Since these three items contribute to space heating, the non-solar internal energy gain was estimated to be the total electrical energy recorded by the power meter.

The building heat loss can be estimated from the building heat loss coefficient (UA) times the difference between the module interior temperature and the ambient air temperature. Therefore, the hourly energy loss for the module can be written as:

$$Qbhl = (UA)(Tr - Ta) \tag{3.15}$$

Equation 3.14 can be expressed as:

$$Qsa + Qsp = Qbhl - Qeh \tag{3.16}$$

There are no south windows in module 6 and shading of the other windows by adjacent buildings reduces the direct passive solar gain. Also, aluminum foil was added to the windows to further reduce this solar passive gain. Indirect passive solar gains due to solar radiation absorbed by the walls and roof are difficult to estimate as the thermal

performance of the components is altered. At any rate, passive gains will result in a reduced conduction energy transfer to the outdoors, or, for large passive gains, a transfer of energy to the module. For module 6, the attic space is well ventilated and the solar collector shades most of the south wall. In addition, a different indirect passive solar gain occurs for each month. Calculation of the effect of the indirect passive solar gain was not possible and its effect on the heating load was assumed to be zero. Then Equation 3.16 can be rewritten as:

$$Qsa = Qbhl - Qeh \qquad\qquad (3.17)$$

To minimize the effect of the indirect passive gains, the building heat loss coefficient (UA factor) in Equation 3.15 was calculated using data in December and January for which little or no bright sunshine hours were recorded. In these months, solar energy is a minimum and the energy for heating the module will come from the heating utility . The UA factor is estimated from Equation 3.17 by neglecting the solar term and the UA equation can be written as:

$$UA = \frac{\sum\limits_{k}^{K} Qeh}{\sum\limits_{k}^{K} (Tr - Ta)} \qquad (3.18)$$

If the whole month of December or January cannot be used as the analysis period, days in each month with little or no solar energy can be used to estimate the UA factor. Then the UA equation can be written as:

$$UA = \left\{ \sum\limits_{m}^{M} \frac{\sum\limits_{i}^{I} Qeh}{\sum\limits_{i}^{I} (Tr - Ta)} \right\} / M \qquad (3.19)$$

Where M is number of days in the analysis month with little or no solar energy .

The monthly total active solar gains (Qmsa) can be computed by:

$$Qmsa = \sum\limits_{k}^{K} Qbhl - \sum\limits_{k}^{K} Qeh \qquad (3.20)$$

And the fraction of total energy for space heating supplied by the active air thermal system is given by:

$$\eta bhl = \frac{Qmsa}{\sum\limits_{k}^{K} Qbhl} = \frac{\sum\limits_{k}^{K} Qbhl - \sum\limits_{k}^{K} Qeh}{\sum\limits_{k}^{K} Qbhl} \qquad (3.21)$$

3.3.2 Solar Contribution Using Power Records Method

Comparing the energy usage by two buildings, module 5 and module 6, is another method for expressing the contribution to space heating by the solar energy system. These two modules have identical construction except for the RSI value of the ceiling insulation level of module 6 which is 63 % greater than that of module 5. Thus, a comparison of electrical energy requirements for each module should indicate the solar contribution for space heating. The power ratio $P\gamma$ of modules 5 and 6 is given by:

$$P\gamma = \frac{\text{Cumulative monthly electric power usage in module 6}}{\text{Cumulative monthly electric power usage in module 5}} = \frac{\sum\limits_{k}^{K} Qeh6}{\sum\limits_{k}^{K} Qeh5} \qquad (3.22)$$

Where

Qeh5 = hourly electric power usage in module 5
Qeh6 = hourly electric power usage in module 6
K   = no. of hours with electric power usage in a month

However, although modules 5 and 6 have identical contruction, the UA factors for these two modules may differ. The power ratio $P\gamma$ of modules 5 and 6 is affected by any deviation of these UA factors and may be compensated for by calculating the power correction factor of these two modules, Fua, under conditions with little or no sunshine. From the discussion of UA factor in section 3.3.1 , the monthly power correction factor can be estimated by using Equation 3.19 for each module.

$$Fua = \frac{\text{Monthly UA factor of module 6}}{\text{Monthly UA factor of module 5}} \qquad (3.23)$$

By combining Equations 3.22 and 3.23 , the monthly actual power ratio can be found as:

$$P\gamma a = P\gamma \ / \ Fua$$

Therefore the monthly fraction of energy for space heating supplied by the solar system can be found as:

$$\eta eh = 1 - P\gamma a \qquad (3.24)$$

3.3.3 Solar Contribution Using F-chart Method

In the development of the computer program called F-chart, assumptions were made that the systems are well-built, flow distribution to collectors is uniform, flow

rates are assumed constant, and the system configurations
will be close to those for which the correlations were
developed[27]. This computer program can be used to predict
the long-term solar heating system performance.

Two dimensionless groups, X and Y, were identified.[27]

$$X = \frac{\text{Ref.collector loss}}{\text{Heating Load}} = \frac{Ac \acute{F}r U^L (Tref - \bar{T}a) \Delta \iota}{L} \qquad (3.25)$$

$$Y = \frac{\text{Absorbed solar energy}}{\text{Heating Load}} = \frac{Ac \acute{F}r (\bar{\tau}\bar{\alpha})\epsilon \bar{H}t.N}{L} \qquad (3.26)$$

Where

Ac	=	collector area, [m²]
Ŕr	=	collector-heat exchanger efficiency factor
U^L	=	collector overall loss coefficient, [W/m²-°C]
Δι	=	total no. of seconds in the month
T̄a	=	monthly average ambient temperature, [°C]
Tref	=	an empirically derived ref. temp., [100 °C]
L	=	monthly total heating load for space heating, [J]
H̄t	=	monthly average daily radiation incident on the collector surface per unit area, [J/m²]
N	=	days in month
(τ̄ᾱ)ε	=	monthly average transmittance-absorptance product

A heat exchanger is not required for an air system. The
term Ŕr is replaced by the solar collector heat removal
factor Fr, and if the duct losses are assumed very small,
Equations 3.25 and 3.26 can be rewritten as:

$$X = FrU^L (Tref - \bar{T}a) \times \Delta \iota \times Ac / L \qquad (3.27)$$

$$Y = Fr(\bar{\tau}\bar{\alpha})\epsilon \times \bar{H}t.N \times Ac / L \qquad (3.28)$$

A dimensionless factor f, called the monthly fraction of heating loads supplied by the solar system, relates these two dimensionless groups X and Y is expressed as follows:

$$f = 1.04Y - 0.065X - 0.159Y^2 + 0.00187X^2 - 0.0095Y^3 \qquad (3.29)$$

The F-chart predictions of solar contribution for the system installed in module 6 were based on the meteorological data obtained from the International Airport and the long-term solar radiation records obtained from Stony Plain about 60 km west of Edmonton.

4. Rating The Thermal System

4.1 Introduction

Many designers and potential users of solar heating systems developed different methods of predicting and measuring the performance of the thermal system. The collector and heat storage facility are the principal components in a solar air-heating system, therefore, their rating is important. Rating can be broadly categorized as:

1. Thermal performance

2. Cost

3. Life time, durability, maintance and ease of installation.

For rating solar air collectors, Kenna[38] pointed out that the rating should take into account the economics and durability factor , together with the thermal performance. The thermal performance of a collector is compared by the concept of collector thermal efficiency and has been studied by a number of investigators, Hottel and Woertz[39], Bliss[40], Whillier[41] and Duffie and Beckman[26][27]. Hill and Streed[33], Löf, Shaw and Oank[17], Siebers and Viskanta[42], and Lunde[8] calculated the performance of solar collector based on meteorological data. A number of reseachers, Klein, Cooper, Freeman, Beckman and Duffie[12], predicted the performance by various theoretical models.

For rating storage beds, the measured and predicted performance of rock bed storage has been studied by Persons,

Duffie and Mitchell[18], Hughes, Klein and Close[19]. A mathematical model was developed for the rock bed and used to study the performance of solar heating systems and cooling systems.

The overall performance of a solar heating system is the result of the thermal performance of the collector and storage bed in conjunction with the control system used. The evaluation of system and component performance will be discussed in this chapter.

4.2 Rating The Solar Air Collector By Thermal Efficiency

The steady state thermal performance of the solar collectors is determined by measuring the energy collected for a combination of values of incident radiation, ambient temperature, and inlet fluid temperature. The performance can be described by an energy balance that indicates the distribution of incident solar energy into useful energy gain and various losses. The energy balance on the collector can be written as:

The rate of useful energy extracted from the collector		The rate of energy absorbed in the collector by the absorber	The rate of energy loss from the collector by conduction, convection and radiation	The rate of energy storage in the collector
	=		−	−

The rate of useful energy extracted from the collector is equal to the rate of energy carried away by the transfer

fluid. If the collector is at steady state, the rate of change of energy storage in the collector materials is assumed to be zero, and the energy balance equation becomes:

$$\frac{\bar{Q}u}{Ac} = Ht(\tau\alpha)\epsilon - U^L(Tp - Ta) = \frac{\bar{m}}{Ac}Cp(Tfe - Tfi) \qquad (4.1)$$

To preclude the necessity for determining the average temperature of the absorber, it is convenient to introduce the parameter Fr, where

$$Fr = \frac{\text{actual useful energy collected by a flat-plate collector}}{\text{useful energy collected if the entire flat-plate collector surface were at the inlet fluid temperature}}$$

Introducing Fr, into Equation(4.1) results in

$$\frac{\bar{Q}u}{Ac} = Fr[Ht(\tau\alpha)\epsilon - U^L(Tfi - Ta)] = \frac{\bar{m}}{Ac}Cp(Tfe - Tfi) \qquad (4.2)$$

This equation is called Hottel-Whillier-Bliss equation (Simth[20]). It expresses heat delivery from a collector in terms of two operating variables:

1. The total (beam, diffuse and reflected) radiation incident on the collector cover plate, Ht, and

2. The temperature between the entering heat removal fluid, Tfi, and the ambient temperature, Ta.

4.3 Governing Thermal Efficiency Equation

The solar collector efficiency is defined as:

$$\xi i = \frac{\text{Actual useful energy collected}}{\substack{\text{Solar energy incident upon or} \\ \text{intercepted by the collector}}} = \frac{\bar{Q}u/Ac}{Ht}$$

According to Equation(4.2), the collector instantaneous efficiency of the flat-plate collector is given by:

$$\xi i = Fr[(\tau\alpha)\epsilon - U^L \frac{(Tfi - Ta)}{Ht}] = \frac{\bar{m}Cp(Tfe - Tfi)}{Ac.Ht} \qquad (4.3)$$

Equation(4.3) indicates that if $Fr(\tau\alpha)\epsilon$ and FrU^L are constant, the plot of ξi versus $(Tfi-Ta)/Ht$ is a straight line with the slope equal to FrU^L and the y-intercept is equal to $Fr(\tau\alpha)\epsilon$.

4.4 Computation Of Collector Thermal Efficiency

The collector efficiency discussed in Section 4.2 and 4.3 is the steady state instantaneous efficiency. However instantaneous readings are impractical because actual thermal systems operate under variable conditions. The thermal efficiency is very sensitive to a sudden change of solar radiation due to cloud, ambient temperature and wind velocity. This suggests that the time averaged collector efficiency over selected periods of time be used in calculations to compensate for the variation in operating

conditions. The collector efficiency is often presented as:

(A) Collector efficiency on an hourly basis

Hourly collector efficiency is selected because it is the minimum time period for meteorological records. The efficiency of the collector during each hour of operation can be found from

$$\xi h = \frac{\bar{Q}u}{Ht.Ac} = \frac{\bar{m}Cp(Tfe - Tfi)}{Ht.Ac} \qquad (4.4)$$

Where Ht is the radiation on the collector titled surface , and $\bar{Q}u$ is the rate of useful energy gain for the hour.

(B) Collector efficiency on a daily basis

The daily efficiency, studied by Duffie and Beckman[26], is not the average hourly efficiency but must be calculated from

$$\xi d = \frac{\sum\limits_{i}^{I} \bar{Q}u}{Ac \sum\limits_{i}^{I} Ht} = \frac{\bar{m}Cp \sum\limits_{i}^{I} (Tfe - Tfi)}{Ac \sum\limits_{i}^{I} Ht} \qquad (4.5)$$

Where $\sum\limits_{i}^{I} \bar{Q}u$ is the total useful energy for the day and $\sum\limits_{i}^{I} Ht$ is the total incident solar radiation on

the tilted surface

(C) Collector efficiency on a monthy basis

Both the hourly and daily efficiency may still be too short a time period to not be affected by the instantaneous meterological conditions. Therefore the monthly collector efficiency has been suggested as the best assessment of the thermal performance of the collector for system design. The monthy efficiency can be calculated by

$$\xi m = \frac{\displaystyle\sum_{k}^{K} \bar{Q}u}{Ac \displaystyle\sum_{k}^{K} Ht} = \frac{\bar{m}Cp \displaystyle\sum_{k}^{K} (Tfe - Tfi)}{Ac \displaystyle\sum_{k}^{K} Ht} \qquad (4.6)$$

Where $\displaystyle\sum_{k}^{K} \bar{Q}u$ is the total useful energy for the month and $\displaystyle\sum_{k}^{K} Ht$ is the total incident solar radiation on the tilted surface.

4.5 The Performance Of The Storage Bin

Althought heat from solar air collectors can be stored in tanks of water or other liquids, in phase-change compounds, in numerous small containers of liquids, and in bins of loose solids, only a pebble bed is technically and economically advantageous[15]. The storage bin is one of the principal components in the solar air-heating system and the

performance of the storage bin will directly affect the performance of the whole thermal system. Therefore, rating the performance of the storage bin is important.

The storage unit for this thermal system is a rock bed with $2m^3$ of washed gravel enclosed in an insulated wood frame box. The energy storage capacity of the bin per area of collector is 545.6 $kJ/m^2-°C$, and the bin can store all of the solar heat collectible on a cloudless day. The storage bin operates in three modes:

1. Collected energy goes directly to the storage bin. This is called heat-collection mode which is symbolized by 'col'.

2. Stored energy from the bin directly supplies the space heating, this is called heat-from-storage mode which is symbolized by 'hfs'.

3. Stored energy from the bin and the electric heater supplies the space heating. This mode is symbolized by 'eh'.

Figure 4.1 shows the schematic diagram for the charging and discharging direction of the storage bin. During charging, the air flows in the downward direction with the air temperature at the top of bin (Tst) higher than the air temperature at the bottom of bin (Tsb). During discharging, the air flows in the upward direction.

From the theoretical conservation of energy point of view, the energy balance on the whole rock bed can be written as:

Heat From
Storage Mode
(Discharging)

Heat
Collection Mode
(Charging)

```
                                                              - - - - - - Tst
                    Storage Bed

                                                              - - - - - - Tsb
```

Heat From Storage
During Electric
Heating Mode
(Discharging)
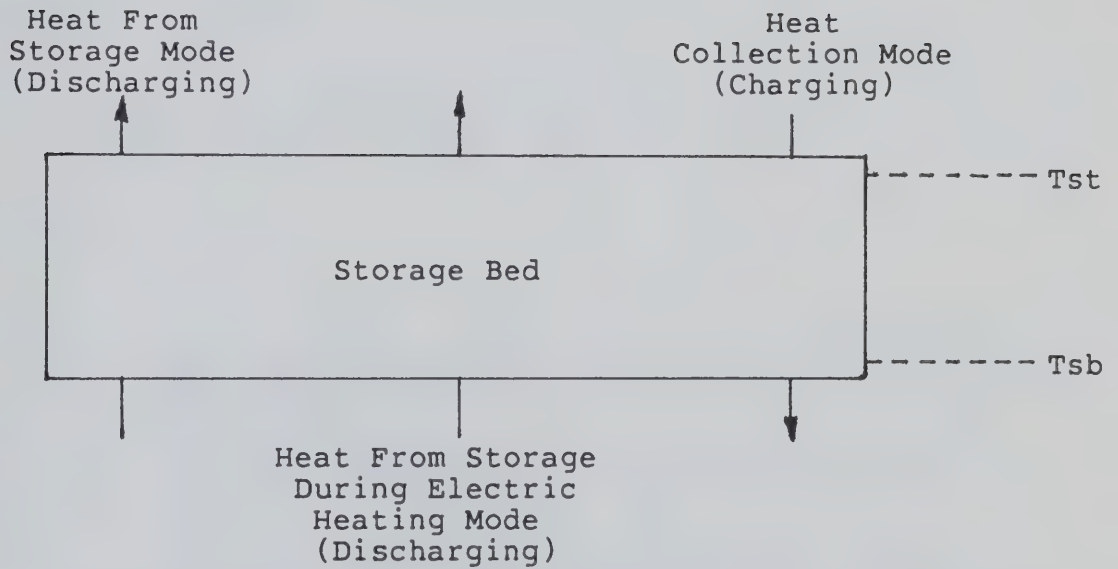
Tst - Air Temperature At The Top Of The Storage Bin

Tsb - Air Temperature At The Bottom Of The Storage Bin

Figure 4.1   Direction Of Charging And Discharging Of The
             Storage Bin Corresponding To Each Operation
             Mode

The rate of energy entering the rock bed − (The rate of energy leaving the bed (include airleakage and conduction through the walls)) = The rate of energy storage in the rock bed

In equation form:

$$\bar{Q}scol - (\bar{Q}shfs + \bar{Q}seh + \bar{Q}sloss) = \bar{Q}sto \qquad (4.7)$$

Where

$\bar{Q}scol$ = rate of solar energy entering the storage bin from collector during heat-collection mode'col', $\bar{m}Cp(DTScol)$, [W]

$\bar{Q}shfs$ = rate of storage energy from the bin supplied for space heating during heat-from-storage mode'hfs', $\bar{m}Cp(DTShfs)$, [W]

$\bar{Q}seh$ = rate of storage energy from the bin for space heating during electrical heating mode'eh', $\bar{m}Cp(DTSeh)$, [W]

$\bar{Q}sto$ = rate of energy accumulated in the storage bin, [W]

$\bar{Q}sloss$ = rate of storage energy losses from storage bin through conduction or air leakage, [W]

The monthly amount of energy loss and storage in the storage bin is:

$$\sum_{k}^{K} Qscol - \sum_{k}^{K} Qshfs - \sum_{k}^{K} Qseh = \sum_{k}^{K} Qsloss + \sum_{k}^{K} Qsto \qquad (4.8)$$

According to the ASHRAE proposed method for the energy balance of the storage bin, the net energy accumulated or

stored inside the rock bin for a monthly period is assumed
to be zero. Therefore, Equation 4.8 can be rewritten as:

$$\sum_{k}^{K} Qsloss = \sum_{k}^{K} Qscol - \sum_{k}^{K} Qshfs - \sum_{k}^{K} Qseh \qquad (4.9)$$

Then

$$Ls = \frac{\text{Monthly energy losses from the bin}}{\text{Monthly solar energy stored in the bin}}$$

$$= \frac{\sum_{k}^{K} Qsloss}{\sum_{k}^{K} Qscol} \qquad (4.10)$$

Equation 4.10 is the fraction of monthly energy lost
from the bin through conduction or air leakage.

4.6 Energy Transfer From Ducts And Storage Bin

Energy losses or energy transfers from the ducts and
storage bin should be determined because they will directly
affect the performance of the thermal system. When the
building requires heating, losses from the storage bin and
ducts that go into the heated space are useful energy
losses. But losses from the duct section located outside the
heated space are detrimental energy losses. In order to

estimate the energy transfers from the thermal system to the module, an energy balance for the module and the thermal system is needed. The monthly solar energy gained from collectors and the monthly total energy required for space heating have been discussed in Chapter 3. The monthly actual solar energy supplied from the thermal system to space heating, Qmas, can be determined by substracting the monthly electrical energy usage from the monthly total energy required for space heating.

$$Qmas = Qmt - Qmeh \qquad (4.11)$$

Then the monthly energy transfers or losses from the thermal system, Qsysl, can be determined by subtracting the monthly actual solar energy (Qmas) from the monthly total solar energy (Qmsun) gained from the collector.

$$Qsysl = Qmsun - Qmas \qquad (4.12)$$

and

$$Łsys = Qsysl / Qmsun \qquad (4.13)$$

Equation 4.13 is the fraction of energy transfers or losses from the thermal system in each month.

5. Results And Discussion

5.1 Introduction

The characteristics of the solar air heating system
were investigated using the methods developed in Chapter 3
and 4. The solar contribution to the heating load was
assessed by direct and indirect methods, the thermal
efficiency of the collector calculated for different time
periods, and the dynamic behavior and the thermal
performance of the storage bin examined. System ductwork and
storage bin energy transfers will also discussed.

5.2 Direct Solar Method

The direct solar method is based on measured energy
quantities to assess the solar contribution. Therefore, the
monthly total number of hours in each system operation mode
is presented in Table 5.1 . Total hours of collector
operation is the sum of hours in heat-from-collector mode
and hours in heat-storage mode. The results indicate that
the bed temperatures are too low for operation in
heat-from-storage mode during December 1981 and January
1982.

The direct solar methods can be divided into 2 parts,
the solar supply method which is based on all the collected
energy supplied by the collector and the solar required
method which is based on the energy required by the module.
Therefore , energy losses are considered in the latter. The

43

44

Table 5.1   Number Of Hours In Each System Operation Mode

Month	Yr	Heat From Collector Mode HFC (Hr)	Heat Storage Mode COL (Hr)	Heat From Storage Mode HFS (Hr)	Electric Heating Mode EH (Hr)	Total Collector Operation HFC+COL (Hr)
Sep	81	29.4	92.2	121.6	27.6	121.6
Oct	81	60.0	39.1	132.6	46.5	99.1
Nov	81	48.2	57.8	67.2	256.7	106.0
Dec	81	72.6	18.1	0.0	359.0	90.7
Jan	82	55.0	5.2	0.0	548.3	60.2
Feb	82	81.8	34.7	11.9	367.7	116.5
Mar	82	60.8	112.0	31.0	238.5	172.8
Season		408.0	359.0	346.0	1844.0	767.0

fraction of energy supplied by the solar system was calculated on a monthly basis and for the heating season. The results are presented in Tables 5.2 and 5.3, and indicate that 11.8 to 15.7 % of total energy was supplied by the thermal solar system for the heating season from September 1981 to March 1982 . The energy supplied to the module is supposedly equal to the energy required by the module. The unequal result for these two methods may be due to the energy losses and energy transfer from ducts and the storage bin.

The solar contribution in the month of September 1981, 62.8 %, was obtained from the supply method while 29.3 % was obtained from the required method. There is a large difference between these two monthly solar contributions. It appears to be due to the fact that September 1981 was a very warm month. The collected energy directly sent to space heating is only about 14.0 % of the energy sent to the storage unit. Also, the energy required from the storage unit for space heating was only about one half of the total energy stored in the bin. The temperature inside the bin was very high and resulted in an increase of energy transfer through the walls of storage bin to the basement. Thus, the large discrepancy between the solar supply method and the solar required method is mainly caused by energy loss from the solar system ductwork and loss from the storage bin.

Table 5.2   Monthly Solar Contribution Assessed By
            Solar Supply Method

Month	Yr	Monthly Electric Energy Qmeh (MJ)	Monthly Incident Solar Qmsun (MJ)	Monthly Heating Load Qmt (MJ)	Percent Solar ηs (%)
Sep	81	1631.3	1473.0	3104.3	62.8
Oct	81	3927.5	904.4	4831.9	19.2
Nov	81	5691.3	982.3	6673.6	14.9
Dec	81	9533.2	871.0	10404.2	8.4
Jan	82	13264.5	669.3	13933.8	4.8
Feb	82	9508.2	1475.0	10983.2	13.6
Mar	82	6418.7	2129.2	8547.9	26.8
Season				58478.9	15.7

Table 5.3   Monthly Solar Contribution Assessed By
            Solar Required Method

Month	Yr	Monthly Electric Energy Qmeh	Monthly Incident Solar	Monthly Heating Load Qmt	Percent Solar ηr
		(MJ)	(MJ)	(MJ)	(%)
Sep	81	1631.3	677.3	2308.6	29.3
Oct	81	3927.5	777.8	4705.3	16.5
Nov	81	5691.3	904.3	6595.6	13.7
Dec	81	9533.2	817.4	10350.6	8.0
Jan	82	13264.5	643.4	13907.9	4.6
Feb	82	9508.2	1315.0	10823.2	12.1
Mar	82	6418.7	1524.6	7943.3	19.2
Season				56634.5	11.8

5.3 Indirect Solar Method

5.3.1 Building Heat Loss Method

The building heat loss method is an alternative method of assessing the solar contribution by using a control volume analysis of the module. The advantage of this method is that the solar contribution can be assessed using a minimum of instrumentation and meteorological data. The parameters used are: the building heat loss coefficient of the module, the room and ambient temperature, and the electrical energy usage. The building heat loss coefficient was calculated to be about 130 W/°C in the month of January 1982, which is the month with little solar energy supplied from the solar thermal system. The solar contribution was assessed by substracting the energy losses from the module from the electrical energy usage and the results are presented in Table 5.4 . During the heating season, 13.8 % of total energy was supplied by the solar system and the monthly solar contribution ranged from 0 to 48.2 %. The zero contribution occurred in January 1982 and appears to be due to damper leakage since the measured solar contribution for January was about 4.6 %. The night time hourly temperature records show that the air temperature at the collector inlet is always greater than the air temperature at the collector outlet. This indicates that leakage is occurring but system configuration did not allow measurement of this leakage.

Table 5.4   Monthly Solar Contribution Assessed By
            Building Heat Loss Method

Month	Yr	Monthly Electric Energy Qeh (MJ)	Monthly Heating Load Qbhl (MJ)	Percent Solar ηbhl (%)
Sep	81	1631.3	3148.6	48.2
Oct	81	3927.5	5519.1	28.8
Nov	81	5691.3	6804.0	16.4
Dec	81	9533.2	10332.4	7.7
Jan	82	13264.5	13226.0	0.0
Feb	82	9508.2	10694.5	11.1
Mar	82	6418.7	8239.4	22.1
Season			57964.0	13.8

The building heat loss coefficient used - 130 W/°C

A low leakage damper on the outlet side of the solar
collector isolates the collector when solar energy is
unavailable. Fan operation during the heating cycle places
the collectors under pressure and any leakage past the
damper introduces cold air into the module. This
characteristic is inherent in the system design and its
effect must be kept to a minimum by good damper seals and
careful adjustment of the control linkage.

5.3.2 Power Records Method

The power records method assesses the solar
contribution by comparing the monthly power usage for module
5 and 6, and then calculating the energy supplied by the
solar system. The heat losses for module 5 and 6 are not
identical, but a correction factor 0.97 (Appendix A-2), was
added to the power equation to adjust for their deviation.
The monthly solar contribution is presented in Table 5.5 .
The table indicates that 11.3 % of total energy was
contributed by the solar system during the heating season,
and the monthly energy saving ranged from 0 to 43.1 % . The
January solar contribution was zero.

5.3.3 F-chart Method

F-chart is a versatile, self-explanatory interactive
computer program developed at the University of Wisconsin
for the analysis and design of active solar heating systems.
Using the parameters of the thermal systems, the

Table 5.5 Monthly Solar Contribution Assessed By
          Power Records Method

Month	Yr	Monthly Electric Power Usage Qeh5 (kW-Hr)	Monthly Electric Power Usage Qeh6 (kW-Hr)	Monthly Power Ratio $P\gamma$ (%)	Percent Solar ηeh (%)
Sep	81	820.7	453.1	55.2	43.1
Oct	81	1612.7	1091.0	67.7	30.2
Nov	81	1939.4	1580.9	81.5	16.0
Dec	81	2851.6	2648.1	92.9	4.2
Jan	82	3577.0	3684.6	103.0	0.0
Feb	82	2887.3	2641.2	91.5	5.7
Mar	82	2372.4	1783.0	75.1	22.6
Season		16061.1	13881.9	86.0	11.3

meteorological data from the International Airport and solar
radiation data from Stony Plain near Edmonton in the
computer program, the long-term average system performance
was calculated and is presented in Table 5.6 . The results
indicate that 17.8 % of total energy was contributed by the
solar system in the heating season, and the monthly solar
contribution ranged from 10 to 44 % .

5.4 Summary Of Solar Contribution Methods

The monthly solar contribution assessed by different
methods for the heating season from Sepember 1981 to March
1982 is presented in Table 5.7 . The results indicate that
the contribution varies from 11.3 % assessed by the power
records method to the 17.8 % contribution predicted by the
F-chart using the meteorological data from the International
Airport and Stony Plain. In Table 5.7 , the solar
contribution 15.7 % calculated from the solar supply method
is higher than the 11.8 % obtained from the solar required
method. That is an expected result because the deviation of
about 3.9 % may be due to the energy losses of the thermal
system. As mentioned in section 5.2 , the contribution of
September 1981 calculated from the supply method is about
62.8 % which is much higher than 29.3 % obtained from the
required method. The main reason for the difference appears
to be the energy tranfers from duct work and the storage
bin. The data indicates that only 14 % of monthly solar
energy collected was used immediately for space heating,

53

Table 5.6   Monthly Solar Contribution Assessed By
            F-chart Method

Month	Yr	Monthly Incident Solar (MJ)	Monthly Heating Load (MJ)	Percent Solar f (%)
Sep	81	4920.0	2800.0	44.0
Oct	81	4840.0	4820.0	31.0
Nov	81	3880.0	7940.0	16.0
Dec	81	3450.0	10680.0	10.0
Jan	82	4310.0	11970.0	12.0
Feb	82	4910.0	9580.0	17.0
Mar	82	6300.0	8870.0	22.0
Season			56660.0	17.8

The Parameters Used: F_rU_L = 2.9 W/m²-°C
                      $F_r(\tau\alpha)_\epsilon$ = 0.5
                      UA Factor = 130.0 W/°C

Collector Flow Rate x Specific Heat / Area = 13.95 W/m²-°C

Storage Capacity Per Area of Collector = 545.6 kJ/m²-°C

Table 5.7   Monthly Solar Contribution Assessed By
            Different Methods

Month	Yr	Direct Methods		Indirect Methods		
		Percent Solar ηs (%)	Percent Solar ηr (%)	Percent Solar ηbhl (%)	Percent Solar ηeh (%)	Percent Solar f (%)
Sep	81	62.8	29.3	48.2	43.1	44.0
Oct	81	19.2	16.5	28.8	30.2	31.0
Nov	81	14.9	13.7	16.4	16.0	16.0
Dec	81	8.4	.8.0	7.7	4.2	10.0
Jan	82	4.8	4.6	0.0	0.0	12.0
Feb	82	13.6	12.1	11.1	5.7	17.0
Mar	82	26.8	19.2	22.1	22.6	22.0
Season		15.7	11.8	13.8	11.3	17.8

while the rest went to the storage unit. However the energy

losses through ducts and walls of the storage unit are very

significant and this will be discussed in section 5.9 . It

shows that the more solar energy collected in the storage

unit, the greater is the deviation between the two methods.

For the indirect methods, the building heat loss method

and the power records method are very similar. Both of these

methods can be used to estimate the solar contribution

without using collector operation and radiation data. The

difference between these two methods is that the building

heat loss method uses the test module as the control module

while the power records method requires a second module

having similar thermal characteristics. The main parameter

of these two methods is the overall building heat loss

coefficient which is difficult to determine but is assumed

to be constant for a specified period. The results obtained

from these two methods for the heating season indicate that

the solar contribution is only 0.5 to 2 percentage points

different from that of solar required method. The solar

energy collected was calculated from records of collector

operation and should be reliable. The January contribution

of about 5 % is reasonable as 60 hours of collection

occurred during this month. It is also acceptable that solar

contribution calculated by the building heat loss and the

power records method was zero during January. Damper leakage

during a cloudy cold January would increase the power

consumption.

F-chart is a theoretical prediction of the long-term solar contribution. The solar contribution of 17.8 % in the heating season obtained from this method is higher than that obtained from the other methods. Both of the F-chart predictions and the solar supply method assumed no energy losses in the thermal system.

The monthly solar contribution for the heating season indicates that:

1. The indirect methods are acceptable methods to assess the solar contribution.

2. Long-term monthly solar assessment by the indirect methods appears to be closer to the actual measured solar contribution.

5.5 Performance Of The Solar Collector

The published performance curves for a solar collector represent its performance under steady state conditions. But solar systems operate under dynamic conditions and the equalities defined by Equations 4.1 and 4.2 do not govern the thermal performance of the collector since part of the solar energy absorbed is used to heat the collector and its components. Because the actual collector performance is under dynamic conditions rather than under steady state conditions, comparison between the actual performance and the steady state performance is necessary.

5.5.1 ASHRAE Standard Test Method

The Solaron 2000 solar collector used on module 6 had been rated using a test method similar to the ASHRAE proposed standard test. But the test data were presented as a plot of collector efficiency versus $(T_{fe}-T_a)/H_t$, where T_{fe} is the air temperature at the collector outlet. Conversions were applied to convert the test result to the standard parameters referenced by Duffie and Beckman[27], $F_r(\tau\alpha)_n$ and F_rU^L, this gave:

1. At normal incidence $F_r(\tau\alpha)_n = F_r(\tau\alpha)\epsilon = 0.5$
2. The collector heat loss factor, $F_rU^L = 2.9$ W/m^2-°C

For an air test flow rate per unit area of collector of 0.0102 m^3/s-m^2, the resulting efficiency curve is shown in Figure 5.1 . With the theoretical performance of the collector known, one may ask, what is the actual performance
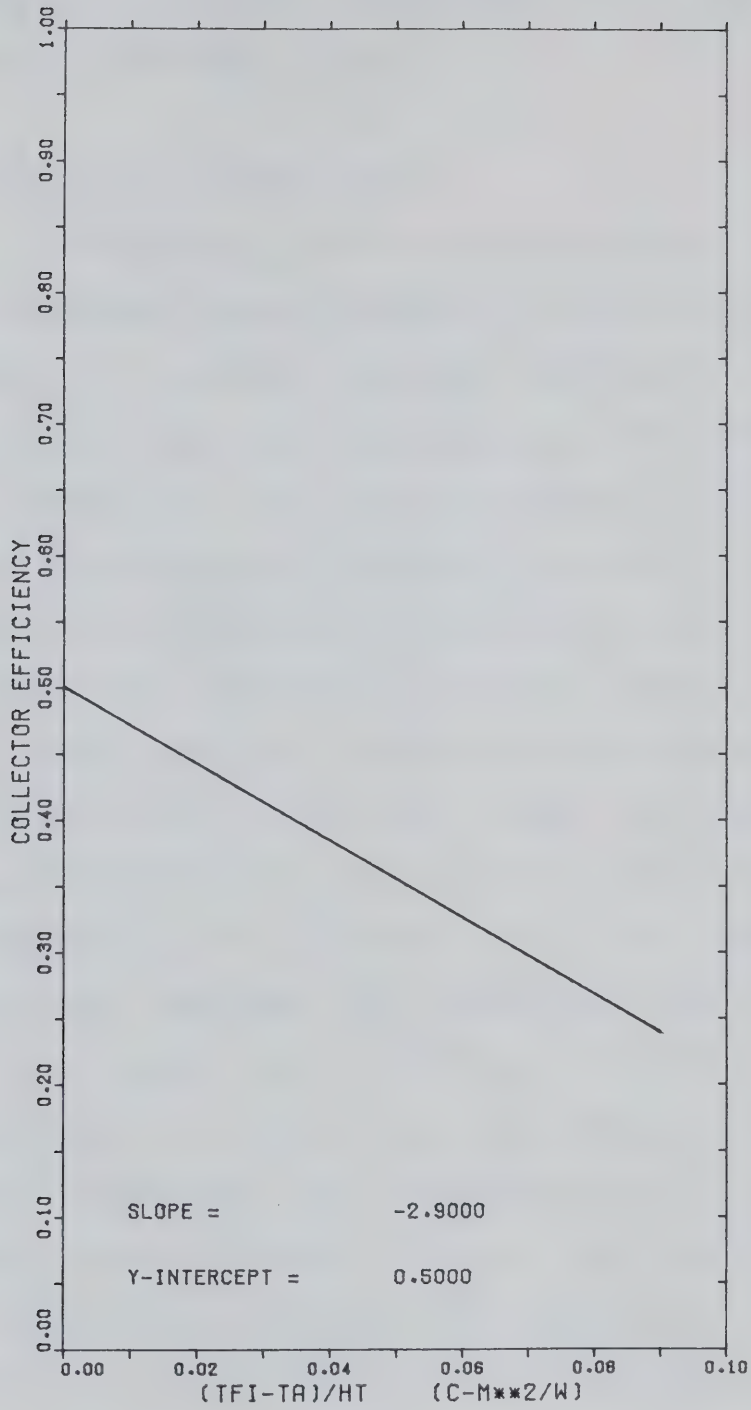
Figure 5.1   Steady State Collector Thermal Efficiency

of the Module 6 collector constructed using these units and
operated in a northern climate?

5.5.2 Instantaneous Efficiency

The instantaneous efficiency of the solar air collector
under a cloudless sky was studied by selecting two days in
March 1982. The collector operated dynamically and the
collector efficiency was calculated for each two minute
interval record over the operation period for that day. The
results are presented in two plots. Figures 5.2 and 5.4
shows collector efficiency versus $(Tfi-Ta)/Ht$. Under steady
state conditions, a straight line should result. Figures 5.3
and 5.5 present the solar radiation on the collector tilted
surface and collector efficiency versus the time of day, and
illustrate the trends of solar radiation and collector
efficiency during the collection period. The number on the
horizontal axis indicates the beginning of the hour.

The efficiency curve in Figures 5.2 and 5.4 may be
separated into two curves. The lower curve sloping upwards
to the left represents the forenoon data with collector
efficiency increasing due to a continuous increase in
radiation during the forenoon. The upper curve sloping
downward to the right represents the afternoon data with the
collector efficiency decreasing due to a continuous decrease
in radiation in the afternoon. The two curves meet at about
solar noon. In theory, these two curves should be the same
for a cloudless day. The reasons for the difference in these
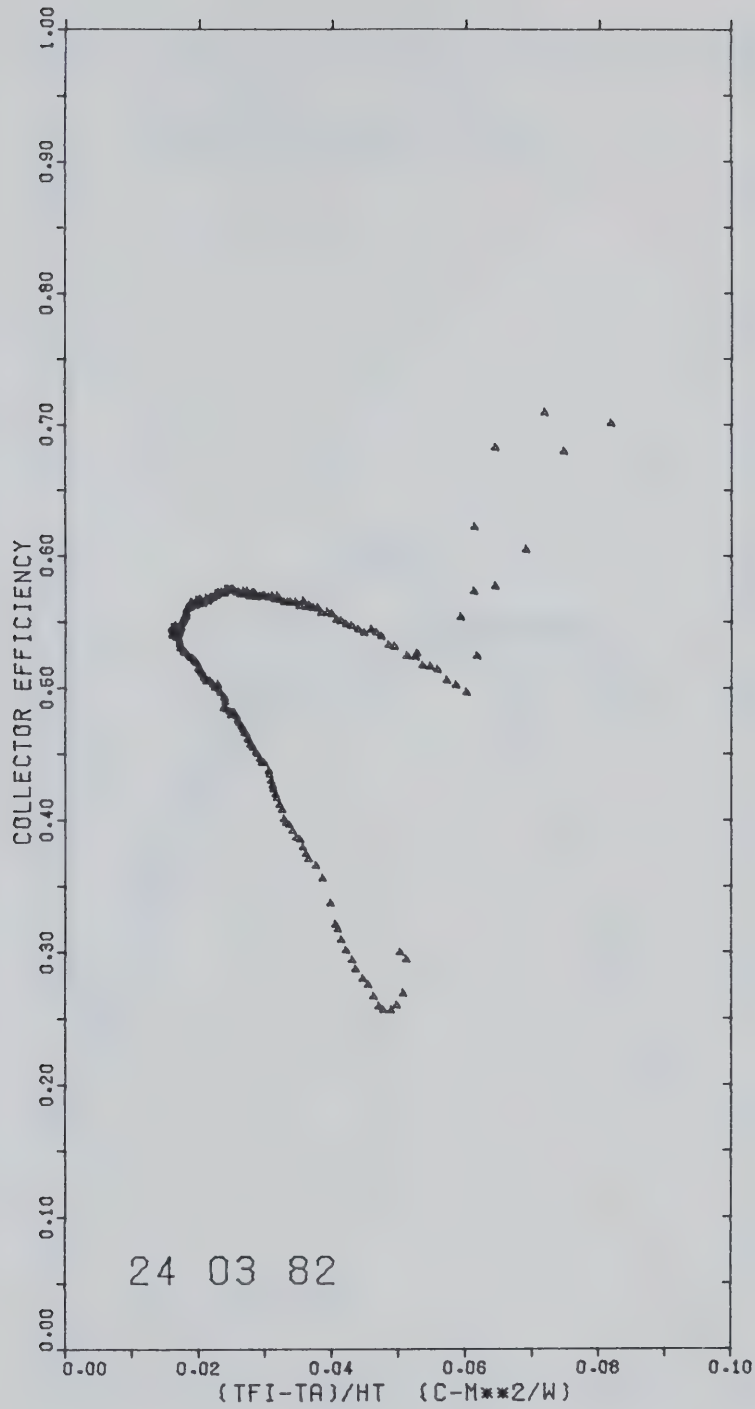
Figure 5.2   Instantaneous Collector Thermal Efficiency
             For 24 March 1982
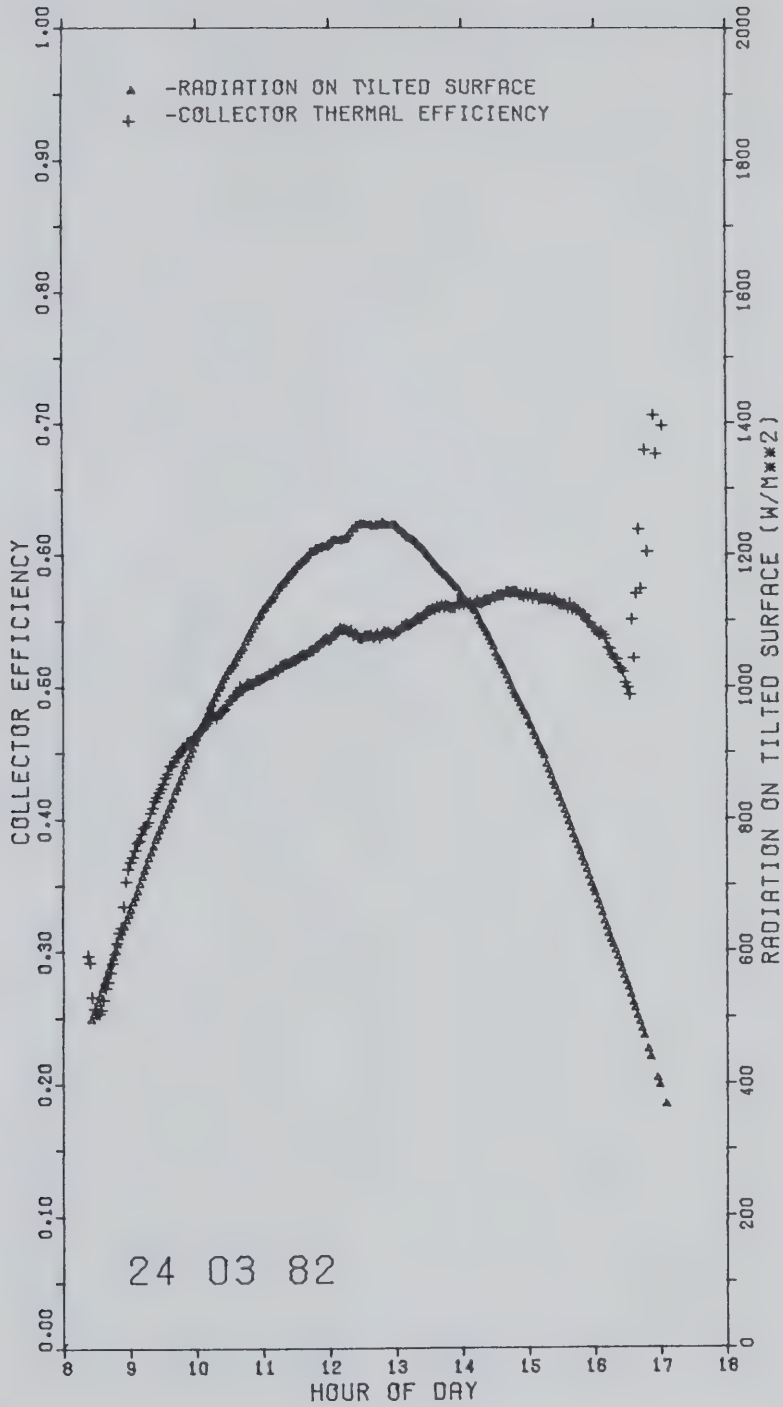
Figure 5.3   Instantaneous Solar Radiation And Collector
Thermal Efficiency For 24 March 1982
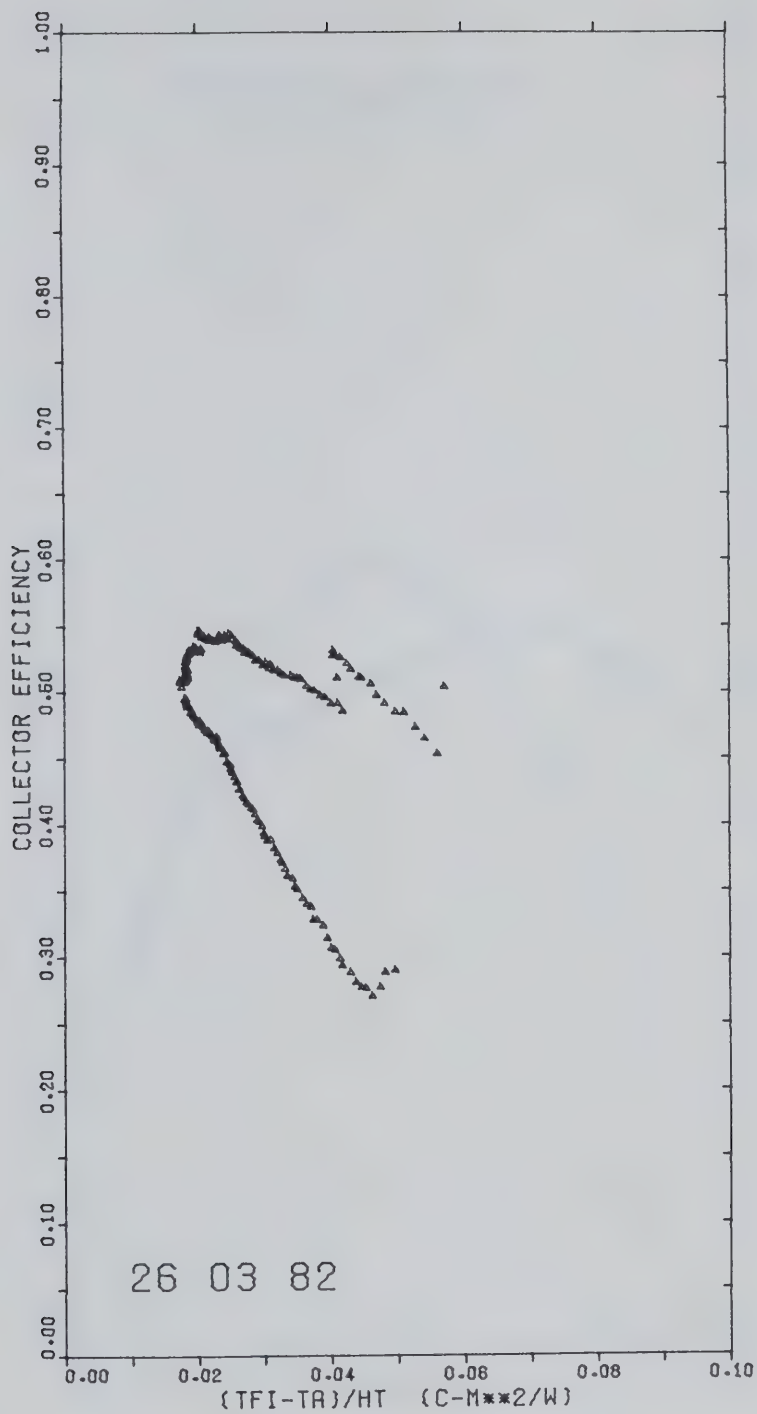
Figure 5.4   Instantaneous Collector Thermal Efficiency
For 26 March 1982
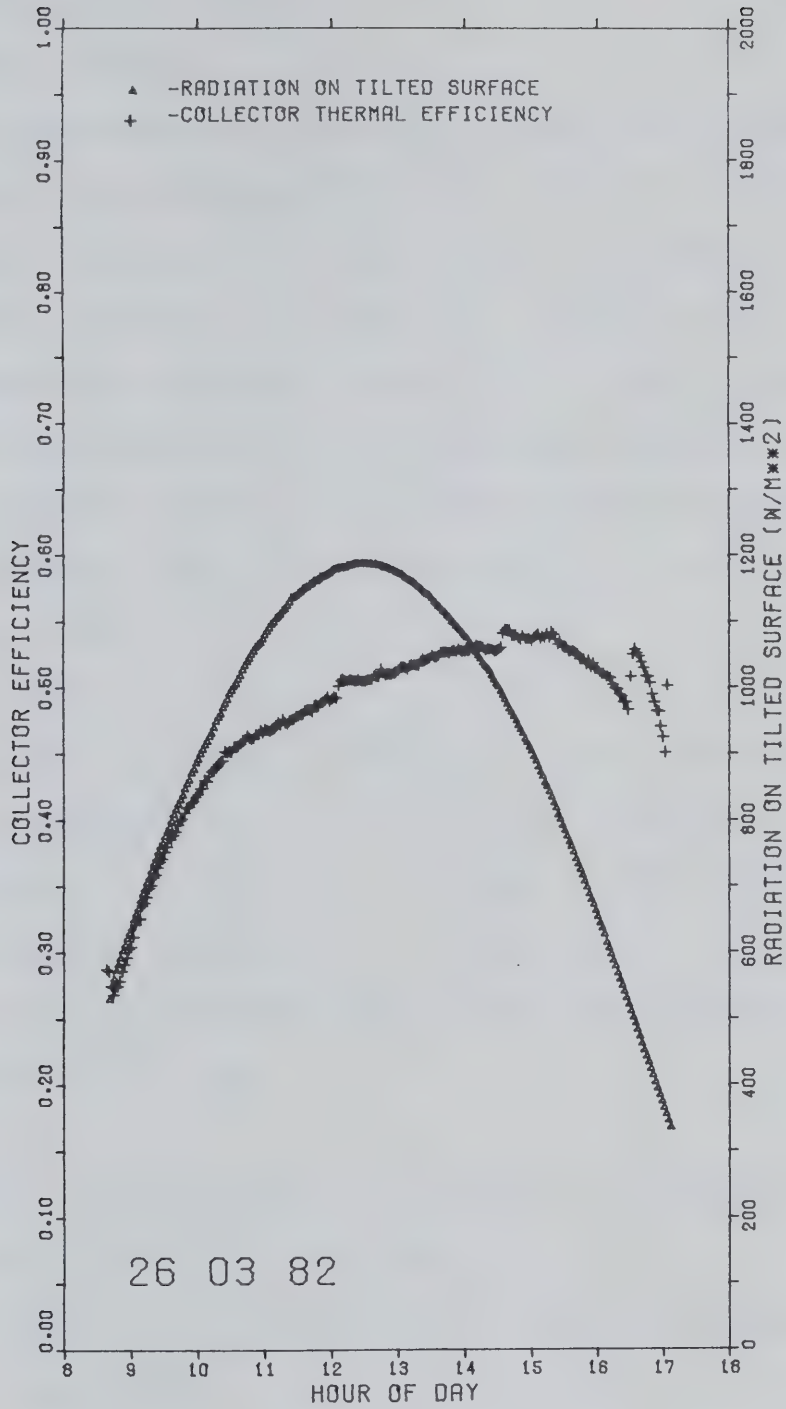
Figure 5.5   Instantaneous Solar Radiation And Collector
             Thermal Efficiency For 26 March 1982

two curves may be due to:

1. Energy storage

    The absorbed energy during the forenoon is partly used
    to heat the components of the collector, so the useful
    energy collected is' lower and the efficiency is lower .
    In the afternoon, as the solar radiation and ambient
    temperature decrease, some of the stored energy appears
    as useful energy and increases the collector efficiency.
    Figures 5.3 and 5.5 also indicate the collector
    efficiency continues to increase for 2 to 3 hours after
    solar noon.

2. Radiation

    The rate of change of radiation during the forenoon and
    the afternoon may not be the same. Figures 5.3 and 5.5
    indicate that the rate of change in solar radiation
    during the forenoon and the afternoon is not the same.
    This should directly affect the efficiency and the
    $(Tfi-Ta)/Ht$ terms.

    Thus, the difference in collector efficiency between
the forenoon and afternoon depends on:

    a. the mass and heat capacity of the collector
        components

    b. the rate of change in solar radiation.

    The unequal length of the forenoon and afternoon curves
appears to be related to the $(Tfe-Tfi)/Ht$ term. Some of the
useful energy used to heat the cold collectors in the early

morning is released during the afternoon. This delays the lowering of the collector exit air temperature and increases the collector operating time. The erratic behavior in efficiency at the end of each curve is due to the on-off cycling of the system at start-up and shut-down.

5.5.3 Hourly Efficiency

In Figures 5.2 to 5.5, the plots of collector efficiency over a day suggest that collector approachs steady state at about solar noon because the rate of change of storage energy in collector approachs zero. In order to investigate this possibility, the records that indicated continuous solar collection for the hour that included solar noon were selected for study. Ideally, only those days with clear sky conditions should be used, but these were few in number, so a combination of clear days and partly cloudy days were used. A plot of hourly collector efficiency at solar noon versus $(T_{fi}-T_a)/H_t$ is presented in Figure 5.6 and the method of least squares was applied to linearize the data. The best fit straight line indicates $F_r(\tau\alpha)\epsilon$ value at about 0.54 and the slope indicates the collector heat loss coefficient at about 1.58 $W/m^2-°C$. The method was repeated using the hour containing solar noon and adding data for the previous and following hour. This gave an $F_r(\tau\alpha)\epsilon$ of 0.53 and an F_rU_L of 1.43 $W/m^2-°C$ in Figure 5.7 . The data exhibits considerable scatter in these two plots, particularly for the larger values of $(T_{fi}-T_a)/H_t$. The major
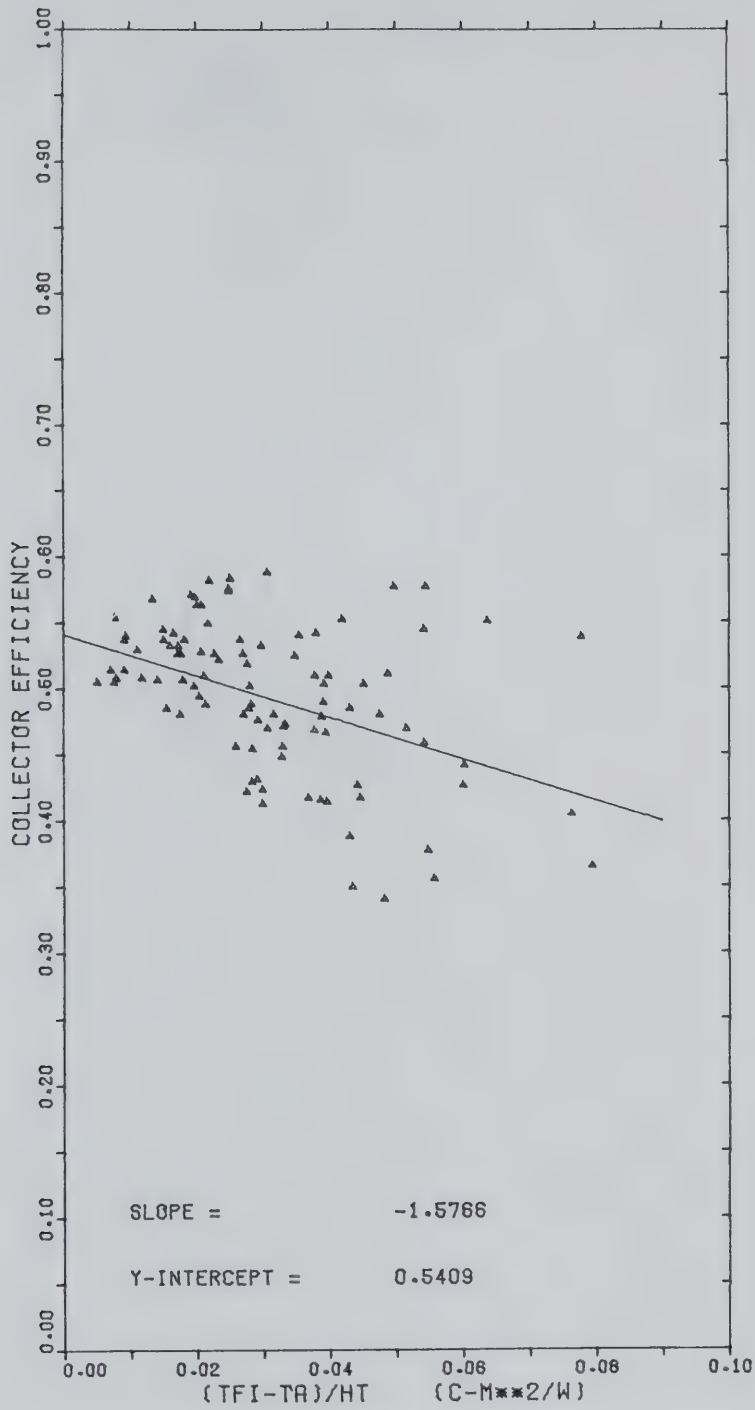
Figure 5.6   Hourly Collector Thermal Efficiency
At Solar Noon
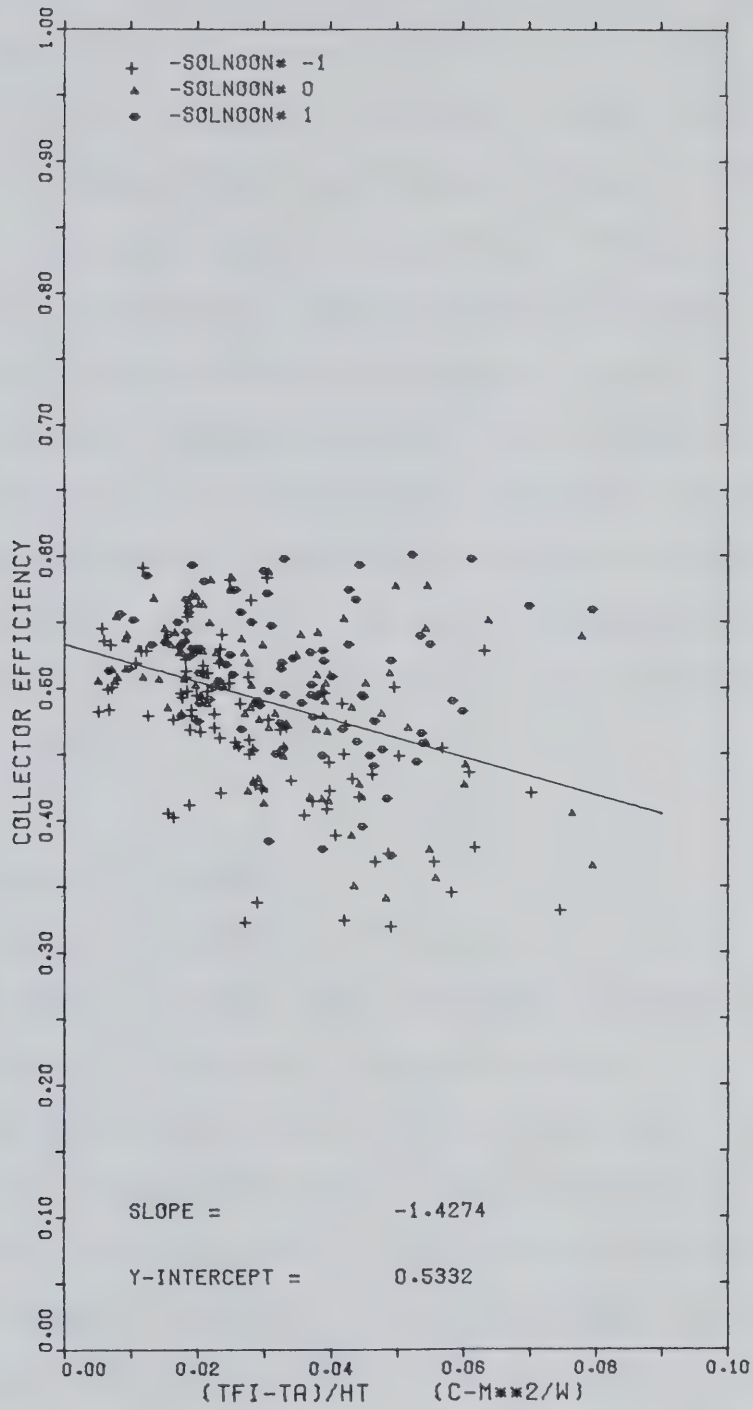
Figure 5.7   Hourly Collector Thermal Efficiency At
            Solar Noon And Including An Hour Before
            And An Hour Thereafter

cause of data scatter is due to clouds that suddenly reduce solar radiation for short periods of time. The (Tfe-Tfi)/Ht or (Tfi-Ta)/Ht term will increase if solar radiation Ht suddenly reduces. But only a small change in (Tfe-Tfi) and (Tfi-Ta) may occur due to release of energy stored in the collector. Therefore, the collector efficiency and (Tfi-Ta)/Ht terms produce erroneous results. On the other hand, the same argument applies for a sudden increase in solar radiation as clouds pass. Therefore, an increase or decrease in radiation shifts the efficiency plot in opposite directions. In addition, the slope represents the heat loss coefficient FrU^L for the collector and is directly affected by data scatter.

5.5.4 Daily Efficiency

A day is the period of a cycle for the collectors to heat up and cool down. Many designers suggest that system performance is related to the performance of the collector for each day. Thus, the collector efficiency on a daily basis was studied. The sum of the useful energy collected, the solar radiation and the temperature difference between the collector inlet and the ambient temperature were calculated on a daily basis. The resulting plot is presented in Figure 5.8 . In this plot, the daily data still shows considerable scatter. After the data is linearized by the least squares method, the best fit straight line indicates an $Fr(\tau\alpha)\epsilon$ of 0.55 and FrU^L of 2.56 W/m²-°C. The scatter of
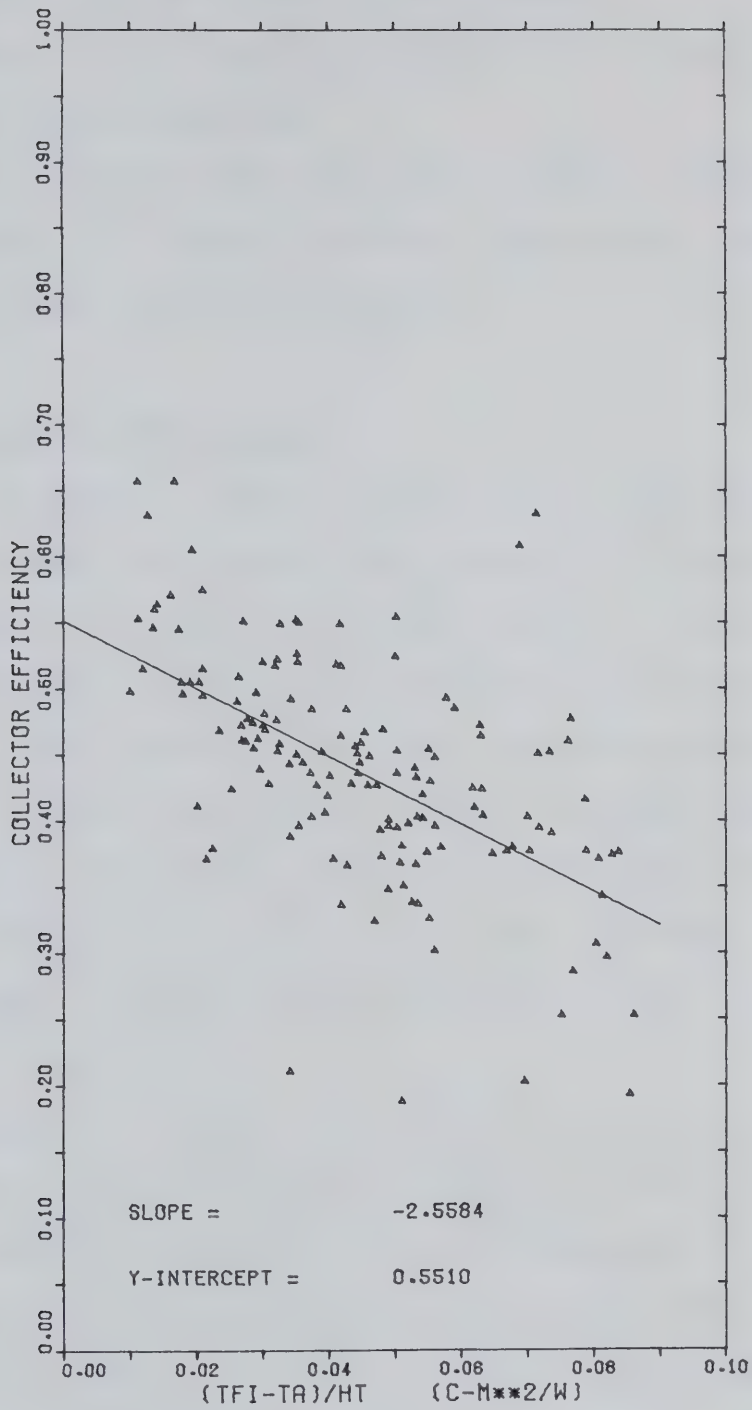
Figure 5.8   Daily Collector Thermal Efficiency

daily data may be caused by two reasons:

1. There may be cloudy periods during the day that reduce
    the solar radiation

2. There may be a few extremely cold and windy days. This
    results in larger collector losses that lower the
    collector daily efficiency

5.5.5 Monthly Efficiency

The plots of instantaneous, hourly and daily basis
suggest that evaluation over a longer time period may be of
assistance in reducing the data scatter. A time period of
one month was selected for study as this period is often
used in calculations. The solar radiation on the collector
tilted surface, the useful energy collected, the temperature
difference between collector inlet and ambient temperature
were calculated for each month. The resulting plot is
presented in Figure 5.9 and gives an $Fr(\tau\alpha)\epsilon$ of 0.56 and
FrU^L of 2.61 $W/m^2-°C$.

Table 5.8 presents the monthly meteorological data and
collector thermal efficiency calculated from solar radiation
and collector air temperature measurements. The normal mean
monthly ambient temperature and the normal hours of bright
sunshine are the long-term average monthly values obtained
from the meteorological records. The R factor is the ratio
of monthly total radiation on a collector tilted surface to
monthly total radiation on a horizontal surface.
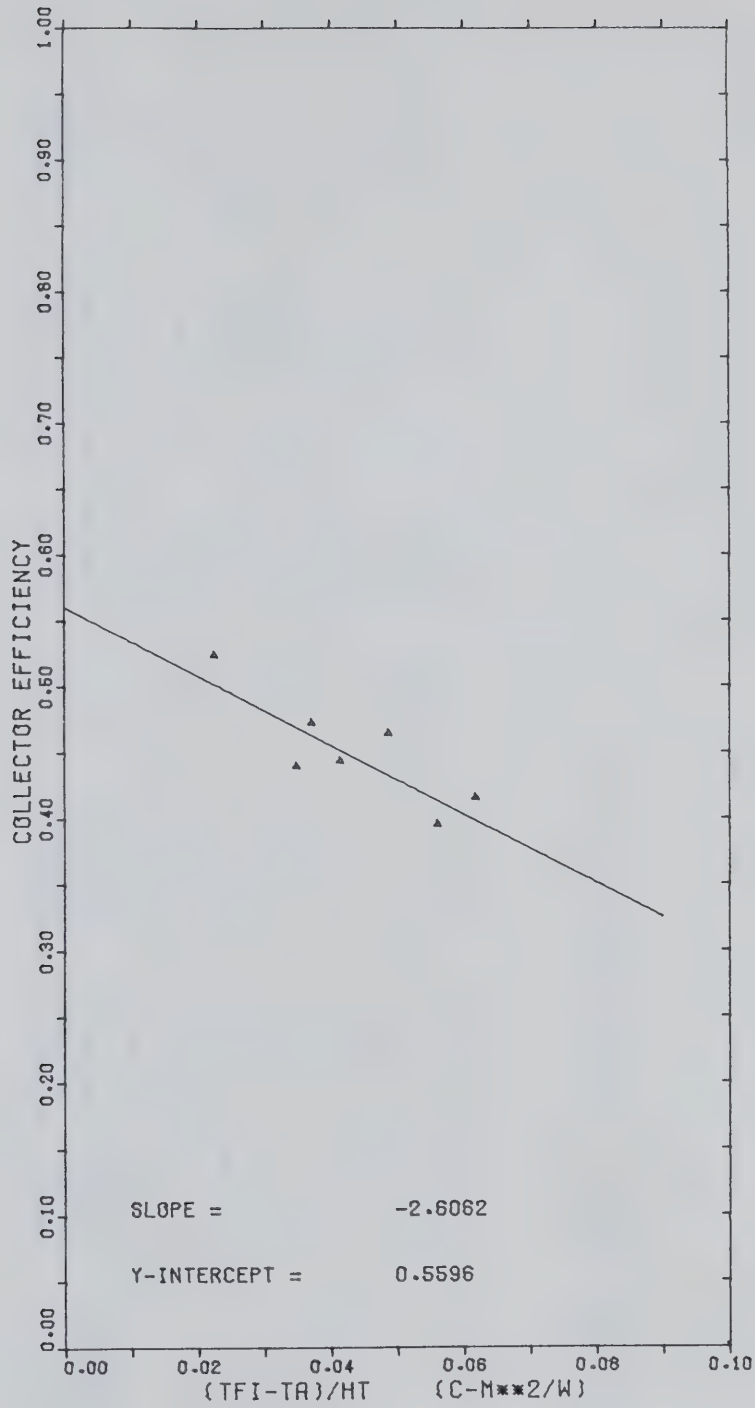
Figure 5.9 Monthly Collector Thermal Efficiency

72

Table 5.8 Monthly Meteorological Data And Collector Thermal Efficiency

Month	Yr	Mean Monthly Ambient Temperature		Hour of Bright Sunshine		Horizontal Surface Radiation	Total Radiation on Tilted Surface	R Factor	Solar Energy Collected	Radiation on Tilted Surface During Collection	Monthly Collector Collection Efficiency
		Actual °C	Normal °C	Actual (Hr)	Normal (Hr)	kW/m²-°C	kW/m²-°C		kW/m²-°C	kW/m²-°C	(%)
Sep	81	10.9	9.7	184	187	87.17	115.47	1.33	54.68	104.94	52.1
Oct	81	2.9	4.2	116	165	58.00	104.47	1.80	27.31	62.48	43.7
Nov	81	-0.9	-5.6	106	97	27.30	67.82	2.48	30.10	68.26	44.1
Dec	81	-10.3	-12.3	96	85	23.02	67.25	2.92	25.99	66.09	39.3
Jan	82	-21.3	-16.3	71	103	24.22	63.67	2.63	21.73	52.62	41.3
Feb	82	-14.2	-12.1	116	113	51.81	108.10	2.09	44.88	97.21	46.2
Mar	82	-6.2	-7.3	134	171	90.85	148.53	1.63	66.53	141.43	47.0

R Factor = $\dfrac{\text{Monthly total radiation on a collector tilted surface}}{\text{Monthly total radiation on a horizontal surface}}$

5.6 Summary For Efficiency Methods

The collector used for module 6 was assembled using 6
Solaron series 2000 flat plate air collectors by connecting
two in series and mounting three of these units in parallel.
This arrangement provided an air heating path length of
about 3.5 m. The dynamic behavior of the collector makes
comparison of the actual collector performance to the
published test performance difficult. Table 5.9 lists the
collector efficiency calculated for the different time
periods. The results indicate that all methods produced
$Fr(\tau\alpha)\epsilon$ values larger than the performance test value of
0.5. Reasons for this may be:

1. The performance test value is determined under steady
    state operation with little or no change in energy
    storage in the collector and with little change in solar
    radiation. Under dynamic conditions, energy storage in
    the collector during the morning results in a steep
    slope for the efficiency curve. During the early
    afternoon, the continuing increase in ambient
    temperature and release of stored energy from the
    collector results in an efficiency curve that first
    increases and then has a low slope for the rest of the
    afternoon. Representing the data by a best straight line
    results in a larger value for $Fr(\tau\alpha)\epsilon$.

2. The accuracy of the data may have been a factor. The
    error in measuring collector flow rate was about 5 %.
    The error in measuring air temperature difference across

Table 5.9   Comparison Of $Fr(\tau\alpha)\epsilon$ And FrU^L
             For Different Methods

	$Fr(\tau\alpha)\epsilon$	FrU^L $W/m^2-{}^\circ C$	
Test	0.5	2.9	
Instantaneous	———	———	
Hourly	0.54	1.58	*
	0.53	1.43	**
Daily	0.55	2.56	
Monthly	0.56	2.61	

*   Data for the hour including solar noon
** Data for the hour including solar noon with one hour
    before and one hour thereafter.

the collector and air temperature difference between room and ambient was about 1.5 %. The solar radiation on the collector tilted surface had an error of about 3 %. Using these error values, the calculated errors for the collector efficiency and the $(T_{fi}-T_a)/H_t$ term were approximately 6 % and 3 % respectively. This produced a 7 to 8 % error in the $F_r(\tau\alpha)\epsilon$ parameter.

The collector heat loss coefficient F_rU_L of 1.43 to 2.61 W/m²-°C is lower than 2.9 W/m²-°C obtained from the rating test. Since insulation had been added to the back of the collector, lower values were expected. In addition, the scatter of the data directly affects the F_rU_L value. For the instantaneous method, energy storage increases during the forenoon and decreases in the afternoon. For clear sky conditions, the solar radiation follows the same pattern, but, when clouds are present, large changes in radiation occur, and this can produce ficticious instantaneous efficiencies that often very low or very large. For the hourly and daily plots, the data scatter indicates the cloud effect is present. The monthly F_rU_L value is probably the more representative of the collector heat losses.

5.7 Dynamic Behavior Of The Rock Bed Storage Bin

Although a number of investigators and storage bin designers have tried many methods of studying the dynamic behaviour of a storage bin, no unique method has been proposed. A bin with 2 m³ of washed gravel is used for energy storage for this thermal system. Due to a shortage of data channels, only the air temperature at the top and bottom of the rock bed were recorded. This selection allowed the calculation of energy added or removed from storage bed. In order to study the dynamic behavior of the storage bin, plots of air temperature at the top of the storage bin and air temperature at the bottom of storage bin versus the day of the week are presented.

Figures 5.10 through 5.16 show the variation in air temperature at the top and bottom of the storage bin during a weekly period for each month. The number on the horizontal axis indicates the end of the day. Figure 5.10 illustrates a period of several days when the bin was overcharged. Figures 5.11 and 5.13 show the bin behavior during a period of low energy storage. Figure 5.14 shows a week when no storage occurred. Figures 5.12, 5.15 and 5.16 show the behavior of the bin when the rock bed temperature wave reached the bottom of the bin during a sunny period.

In Figure 5.15, the third week of February 1982, the results for February 15th indicate that there is no energy storage inside the bin, therefore, the temperature gradient across the bin is zero. The plot also indicates that there
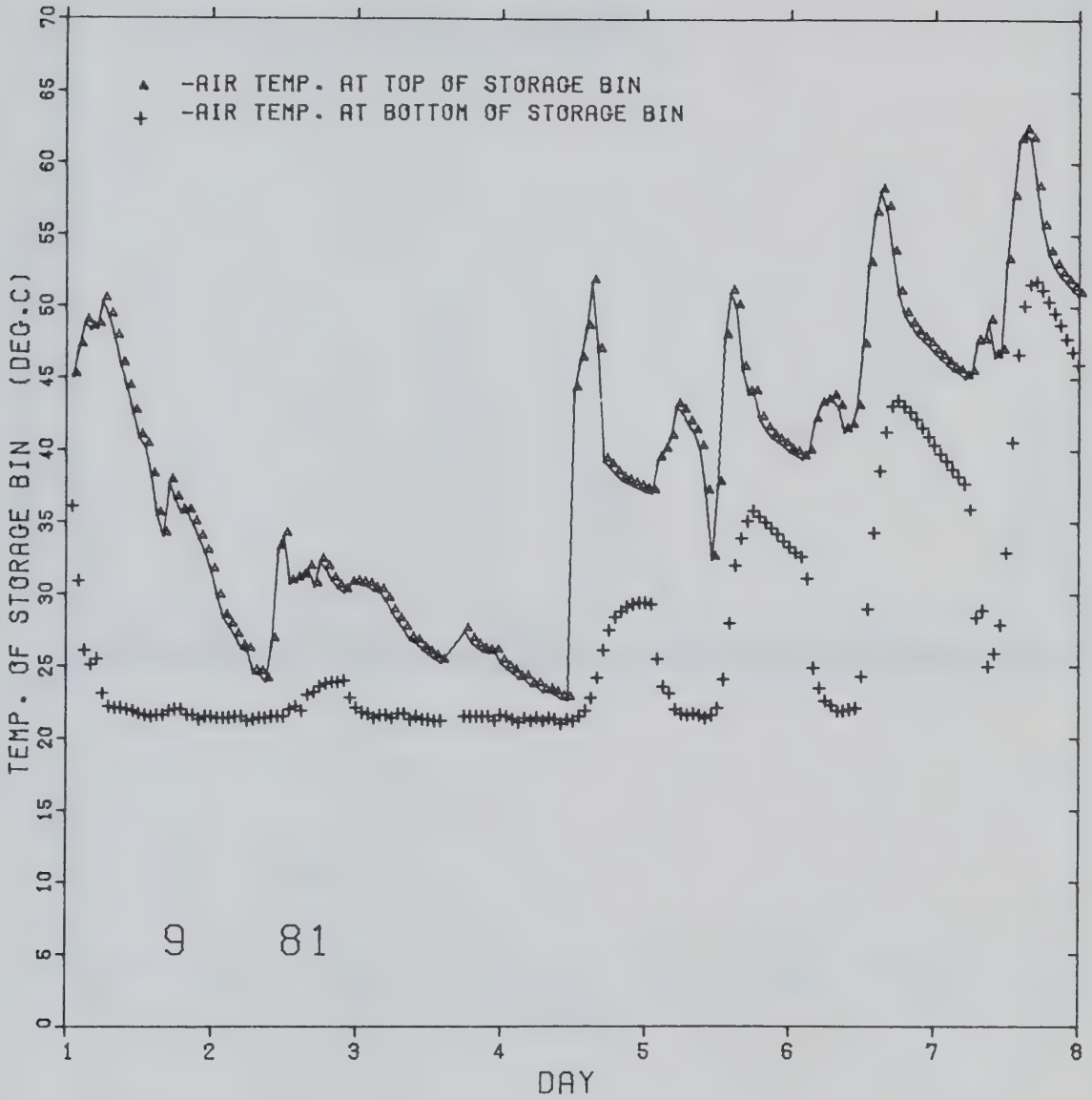
Figure 5.10   Air Temperature At Top And Bottom Of The
              Storage Bin For The Week Of 2 To 8,
              September 1981
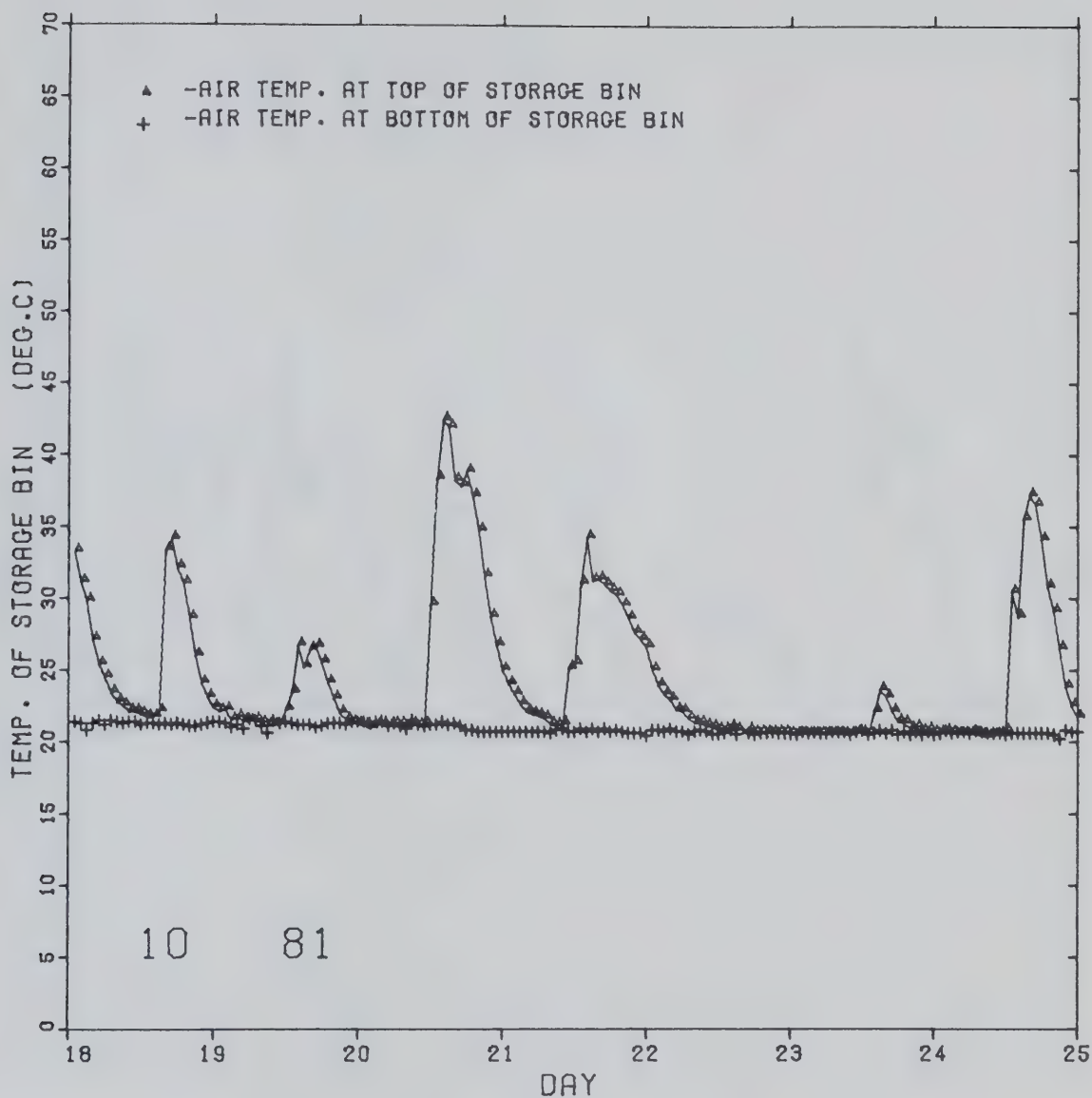
Figure 5.11   Air Temperature At Top And Bottom Of The
              Storage Bin For The Week Of 19 To 25,
              October 1981
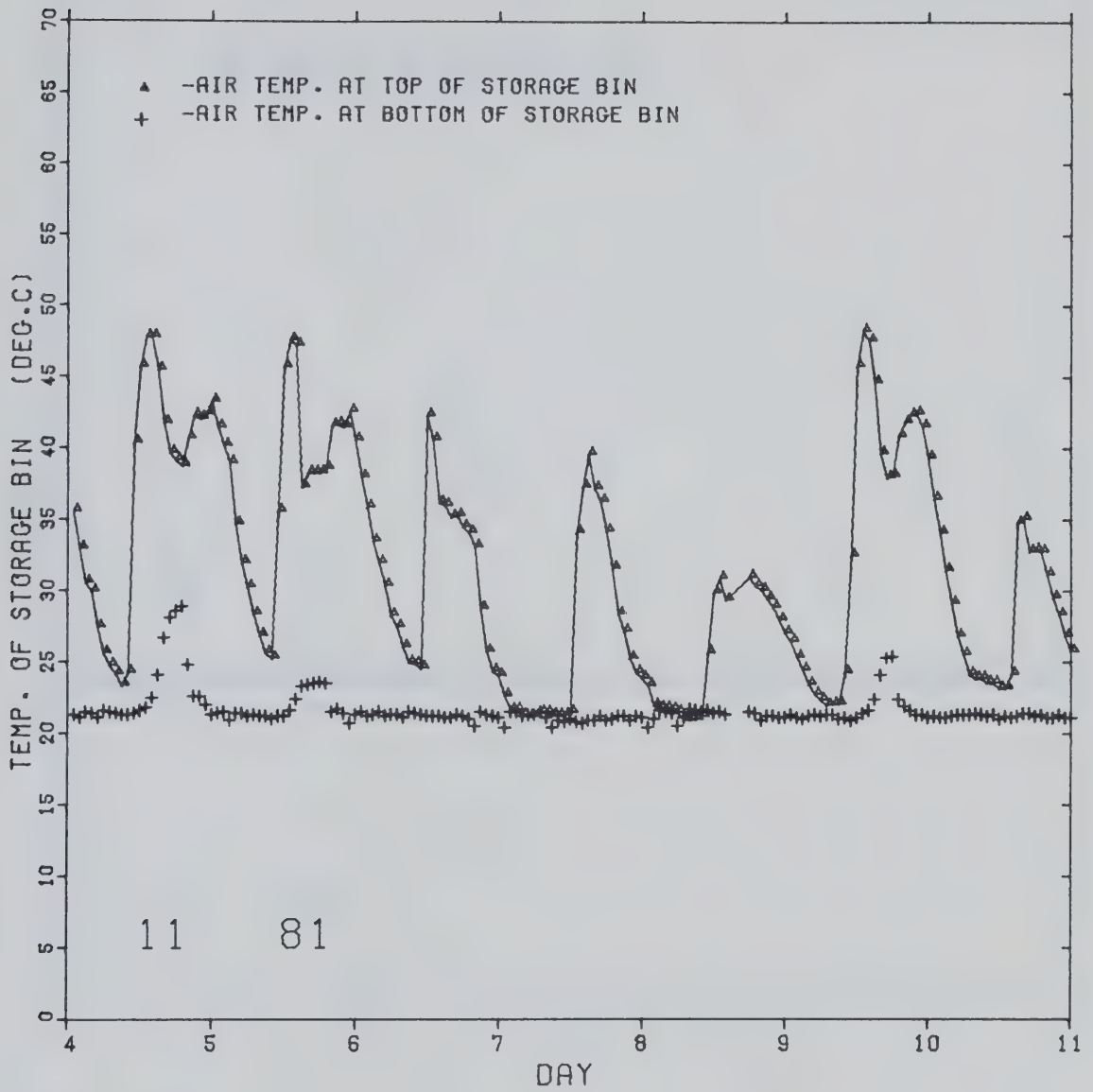
Figure 5.12   Air Temperature At Top And Bottom Of The
             Storage Bin For The Week Of 5 To 11,
             November 1981
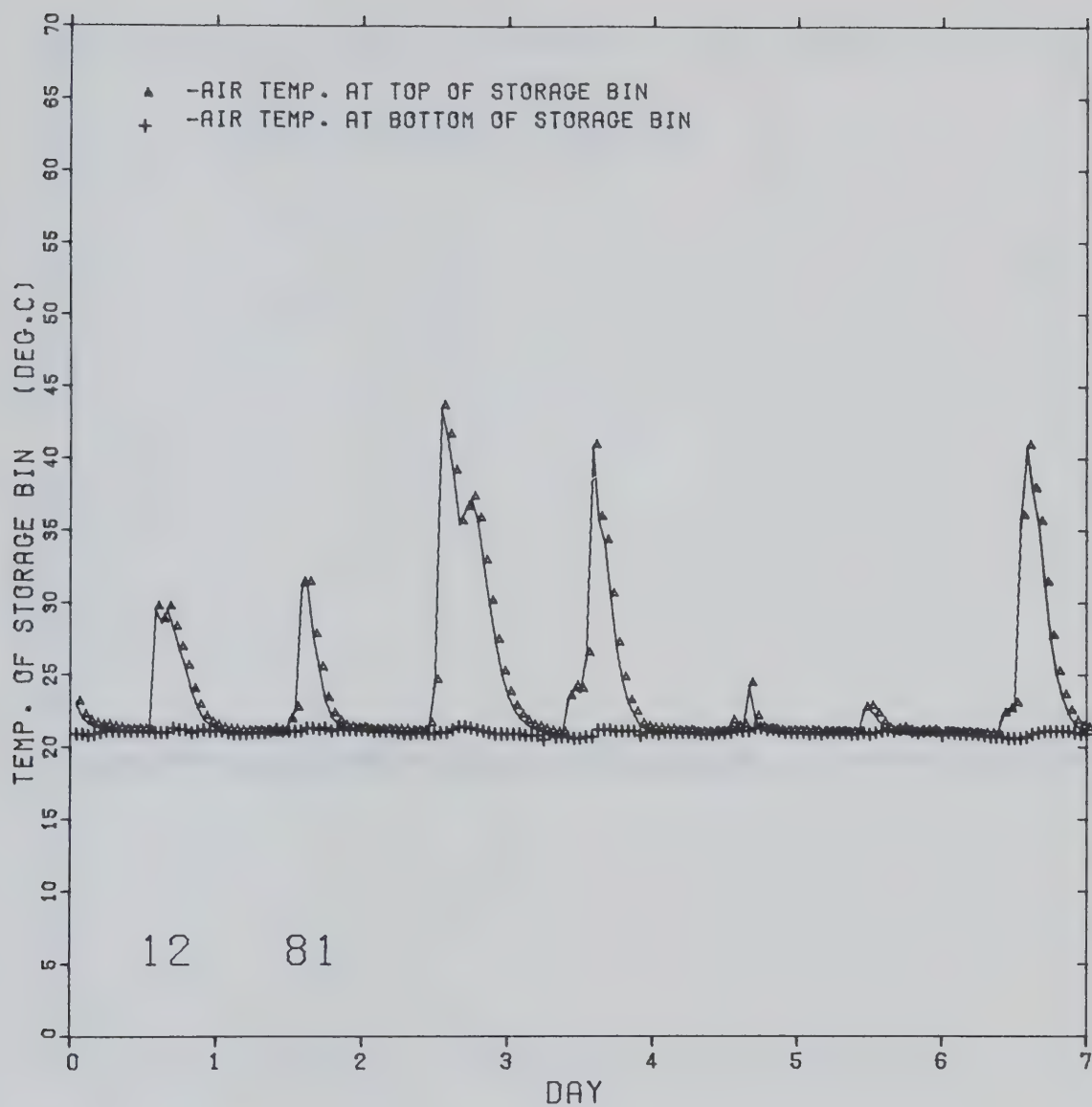
Figure 5.13   Air Temperature At Top And Bottom Of The
              Storage Bin For The Week Of 1 To 7,
              December 1981
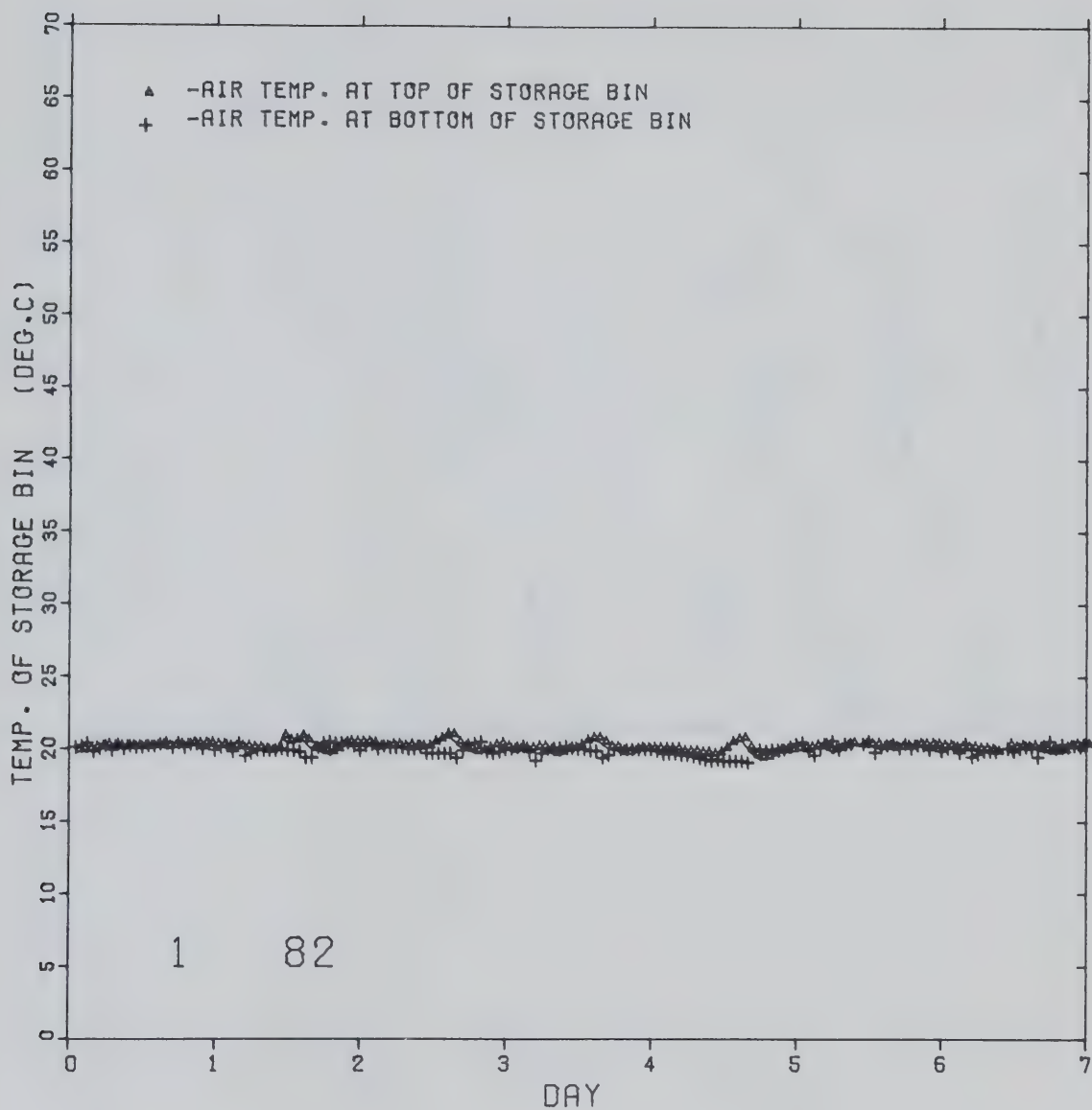
Figure 5.14   Air Temperature At Top And Bottom Of The
              Storage Bin For The Week Of 1 To 7,
              January 1982
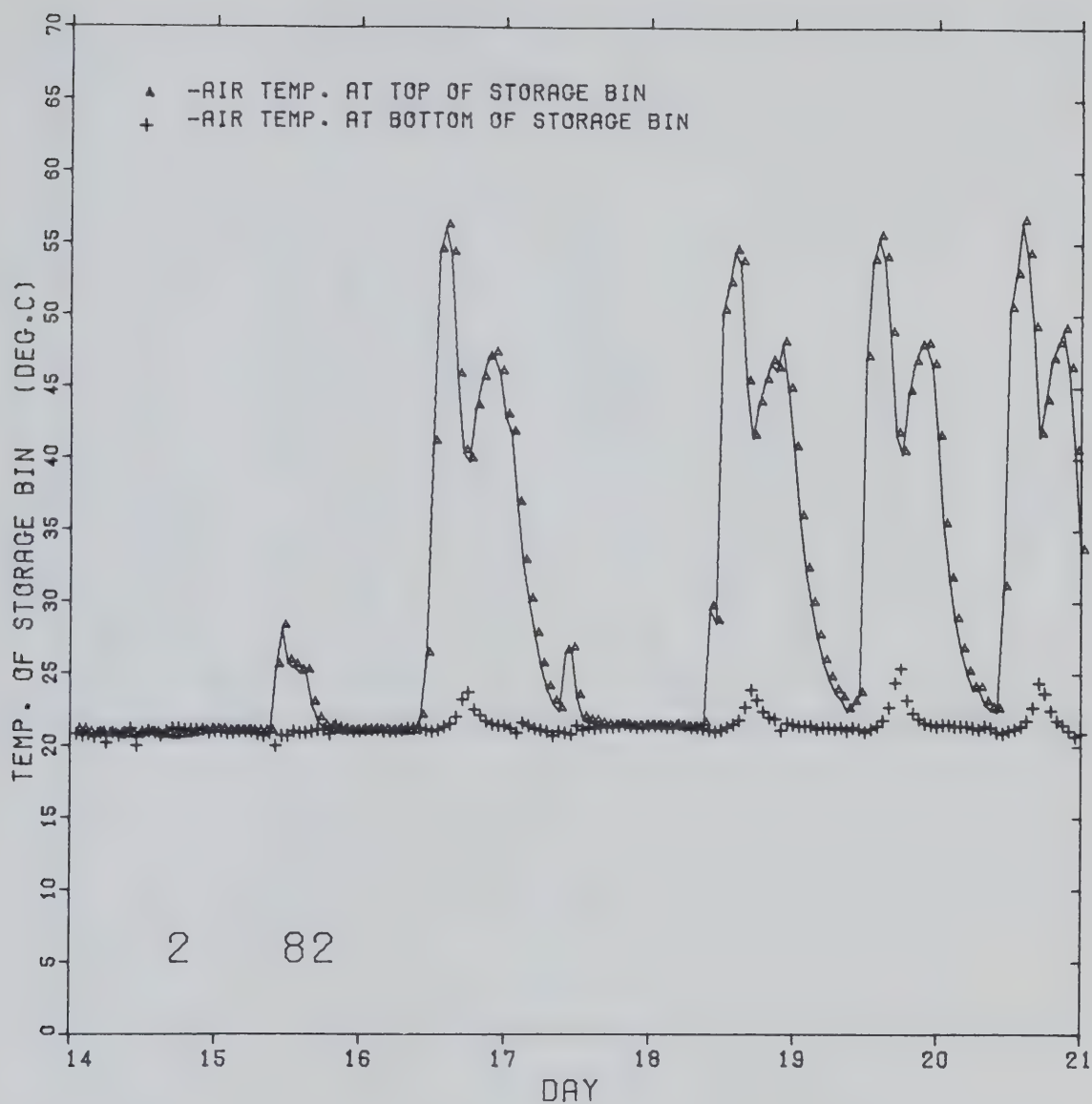
Figure 5.15   Air Temperature At Top And Bottom Of The
              Storage Bin For The Week Of 15 To 21,
              February 1982
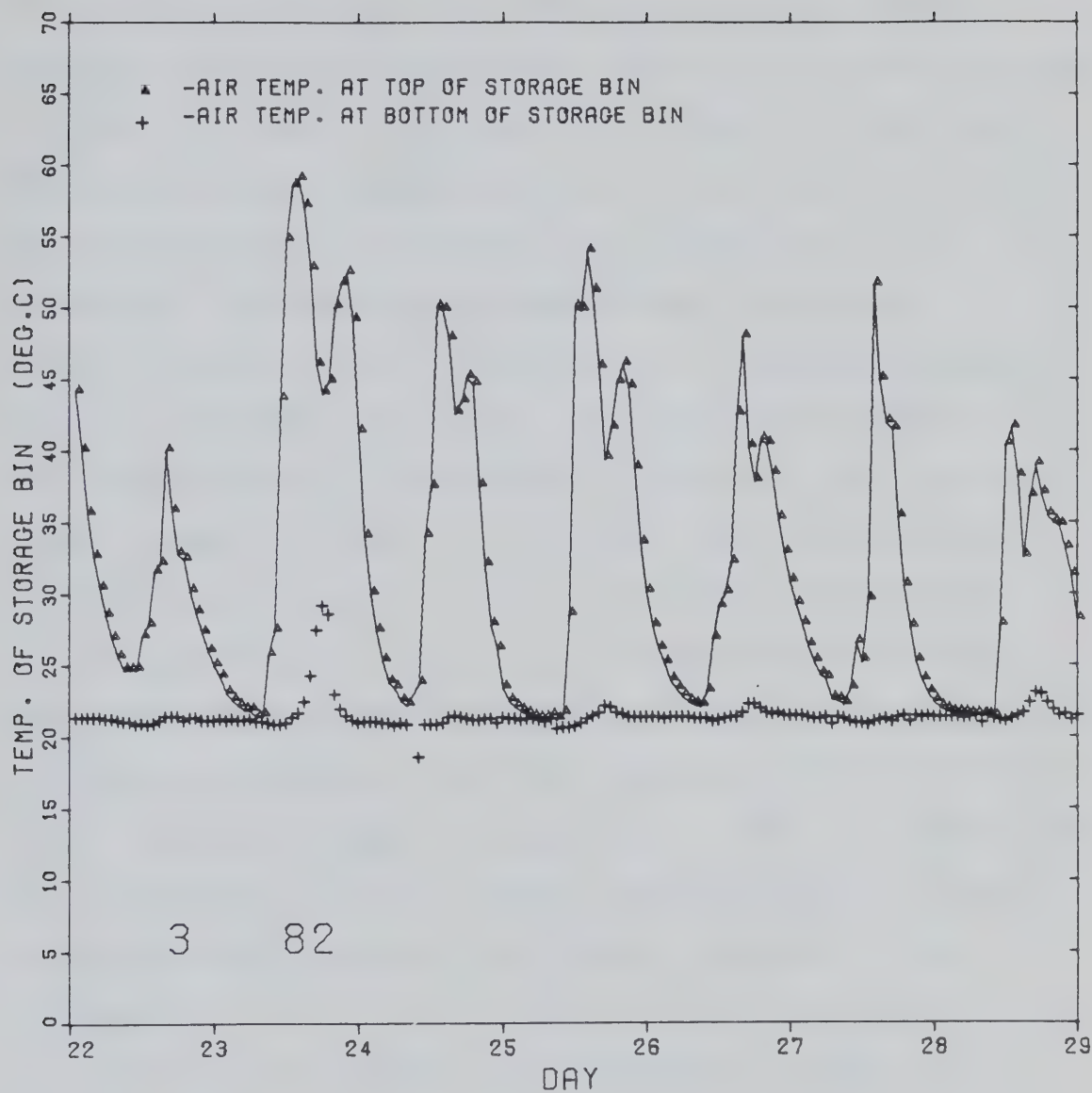
Figure 5.16   Air Temperature At Top And Bottom Of The
              Storage Bin For The Week Of 23 To 29,
              March 1982

is little solar energy stored in the bin during days 16 and
18 of February. This may be due to cloud effect or that any
solar energy collected was used immediately for space
heating. Figure 5.15 shows that there are two peaks for days
17 and 19 through 21 of February. In order to have a more
detailed study of dynamic behaviour of the rock bin, a plot
of air temperature at the top and bottom of the bin,
collector inlet and outlet temperature, and ambient
temperature versus the time of day for 2 consecutive days,
20 and 21 of February of 1982, is presented in Figure 5.17 .
The system operation modes are also shown on the top of the
plot. Figures 5.15 and 5.17 indicate that the maximum air
temperature at the top of the bin occurred shortly after
noon, decreased to about 40 °C, increased again to about
48 °C when the system switched to the heat-from-storage mode
in the late afternoon, and then continually decreased until
solar collection began the next morning. The air temperature
at the bottom of the bin remains nearly constant at about
room temperature except a few degrees increase in the
afternoon.

During the forenoon, the temperature of the air
entering the bin continuouly increased and a temperature
gradient was established throughout the bin. The top of the
rock bin would be approaching the air temperature. Shortly
after solar noon, the air delivered to the bin was at a
lower temperature than the top of the rock bin. This air
would start to cool the top of the rock bed, and while no
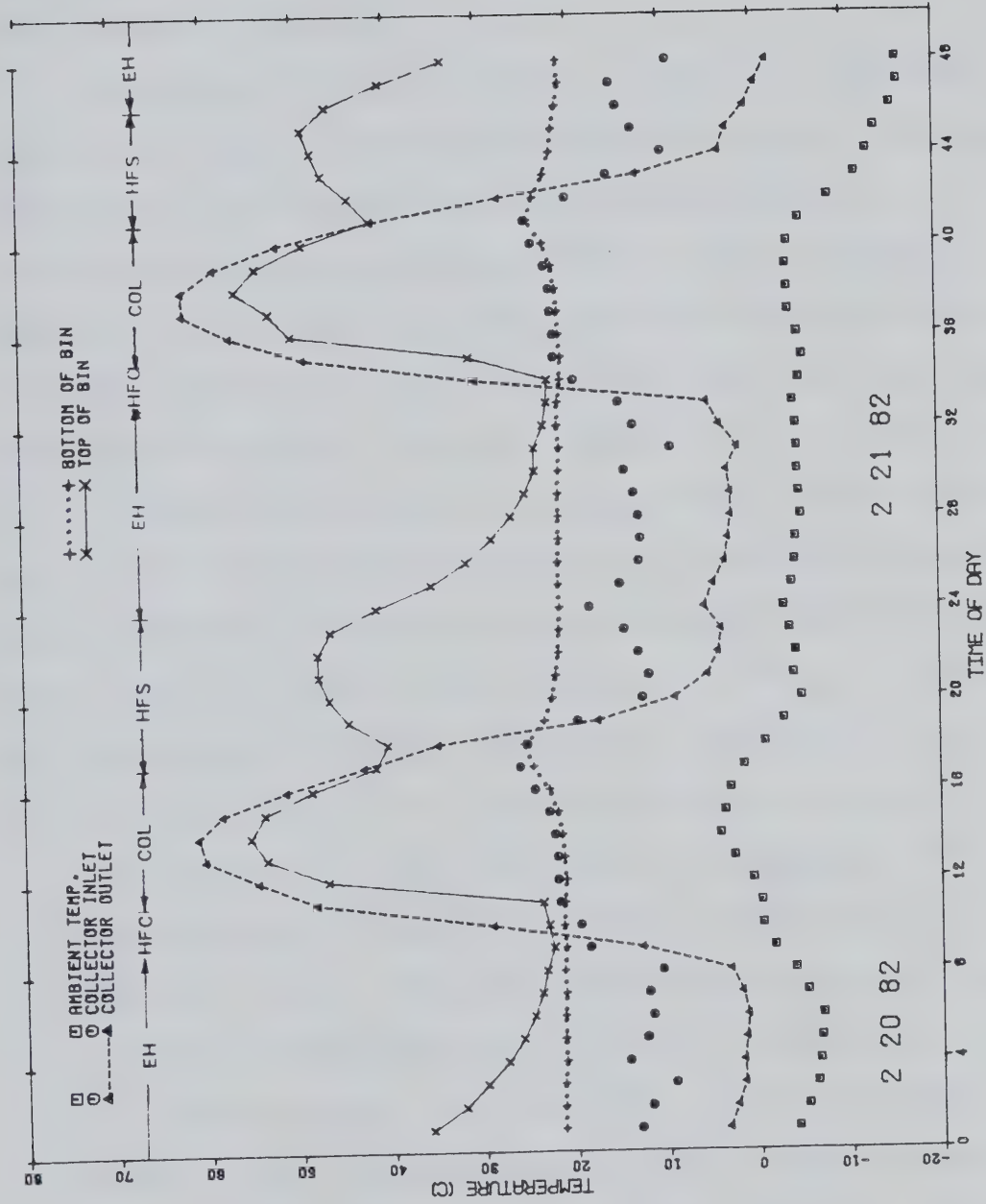
Figure 5.17 Performance Of The Active Air Thermal System On
2 Consecutive Days, 20 And 21 February 1982

energy was lost, the energy was carried to lower levels of the bin. In this way, a temperature wavefront propagated slowly through the bin. Eventually, this wave would reach the bottom of the bin and increase the air temperature at the bottom of the bin.

Temperature data presented in Table A-1 (Appendix A-1) shows that space heating was required at about 1700 hour. The result shows that no energy was available from the collectors but energy was available in the storage bin, therefore the system operation mode switched from the heat storage mode to the heat-from-storage mode with air flow in the upward direction. The air temperature at the top of the bin increased due to the high temperature in the centre portion of the bin and decreased as the stored energy was used. Therefore, the first peak that appeared shortly after solar noon was due to solar energy sent directly to storage, and the second peak that appeared in the evening was due to the storage energy in the bin during space heating.

In Figure 5.11, the first week of September 1981, this plot shows that the bin was very hot during days 5 through 8 of September. Also, the peaks appearing in each of these days are different from days 20 and 21 of February 1982. During days 5 through 8 of September, the first peak appearing in the early morning was due to the storage energy in the bin being used for during space heating , and the second peak appearing at about solar noon was due to solar energy during energy storage.

5.8 Performance Of Storage Bin

The storage bin is one of the principal components of the thermal air heating system, therefore the performance of storage bin should directly affect the performance of the thermal system. The heat transfers from the walls of the bin should be minimized not only to increase the performance of the thermal system but also to avoid overheating the module in the summer. The rock bed temperature stratification and behavior of the bin components could not be studied with the available instrumentation. Instead, the monthly energy flows to and from the bin were calculated to estimate the energy loss for the bin.

Table 5.10 shows that the monthly energy transfers and the losses from the storage bin through air leakage or wall conduction. During the heating season from September 1981 to March 1982, 834.6 MJ of energy were lost from the storage bin through wall conduction or air leakage. This was 23.6 % of the total solar energy stored in the bin. The losses are high but still acceptable. It is interesting to note that there are little loss in the months of November 1981 through January 1982. This is due to little solar energy stored in the bin and the temperature inside the bin is nearly equal to the space(room) temperature. There are 34.8 % and 30.7 % energy losses in the months of September 1981 and March 1982 respectively.

During the heating season, the energy lost through the walls and top of the bin contributed to heating the module.

Table 5.10 Monthly Energy Loss From The Storage Bin

Month	Yr	Monthly Energy Storage Qscol (MJ)	Monthly Heat From Storage Qshfs (MJ)	Monthly Storage With Electric Qseh (MJ)	Monthly Storage Bin Loss Qsloss (MJ)	Percent Loss Of Stored Energy Ls (%)
Sep	81	757.4	467.0	28.6	263.3	34.8
Oct	81	364.4	281.6	37.0	75.8	21.8
Nov	81	546.0	253.5	285.0	20.0	3.7
Dec	81	145.5	0.0	143.8	1.7	1.2
Jan	82	44.8	0.0	42.9	1.9	4.2
Feb	82	419.5	152.1	178.7	88.7	21.1
Mar	82	1247.7	369.3	501.1	383.5	30.7
Total		3525.3			834.6	
Season						23.6

Monthly Qscol = Monthly energy entering the storage bin from
               collector during heat-collection mode

The rock bed was constructed on the basement floor and the lower air plenum was insulated from the basement floor by 50.8 mm of rigid insulation. Since the measured average hourly air temperature for the lower plenum was about equal to room temperature, the loss through the bottom of the bin would be equivalent to the loss of basement floor insulated with 50.8 mm of rigid insulation. Measured basement floor losses were about 4 W/m² and remained almost constant throughout the year. Correction for the added insulation gave an estimated energy loss of about 7.5 MJ/month.

Table 5.11 shows that the monthly energy losses from the storage bin including the losses of the duct section between the collectors and storage bin. A total of 1805.8 MJ which represents about 39.9 % of the total solar energy delivered to the bin was lost or transfered to the space during this heating season. By comparing with Table 5.10 , the results show that the losses or energy transfers in September 1981 increased from 34.8 % to 61.7 %. It was not possible to separate the indoor and outdoor duct losses, but comparison with Table 5.10 indicates that the monthly duct losses for October to March varied from about 8 to 22 % of the collected energy that was delivered to storage. The larger values occurred during December and January. During cold months, an increase in loss occurs for the outdoor ducts. A large loss for September 1981 results due to the storage bin being overcharged and high collector outlet temperature occurring during the heat collection period.

Table 5.11   Monthly Energy Loss From Storage Bin
             Including The Duct Loss

Month	Yr	Monthly Collected Energy To Storage Qccol (MJ)	Monthly Energy From Storage Qshfs (MJ)	Monthly Storage With Electric Qseh (MJ)	Monthly Storage Loss Qsloss (MJ)	Percent Of Storage Loss (%)	Solar Loss (%)
Sep	81	1289.3	467.0	28.6	795.1	61.7	54.0
Oct	81	415.1	281.6	37.0	111.2	26.8	12.3
Nov	81	616.3	253.5	285.0	77.8	12.6	7.9
Dec	81	187.1	0.0	143.8	43.3	23.1	5.0
Jan	82	57.0	0.0	42.9	14.1	24.7	2.1
Feb	82	490.7	152.1	178.7	159.9	32.6	10.8
Mar	82	1469.7	369.3	501.1	604.5	28.4	28.4
Total		4525.2			1805.8		
Season						39.9	21.5

Monthly Qccol = Monthly energy delivered from collectors to
                storage bin during heat-collection mode

Percent of Storage Loss = Percent of storage loss to the
                          total collected energy delivered
                          to the bin

Percent of Solar Loss   = Percent of storage loss to the
                          total collected energy

5.9 Energy Transfers From The Thermal System

Table 5.12 shows the monthly energy transfer or loss of the whole thermal air system. The results indicate that in total 1838.7 MJ, which is about 21.9 % of the total solar gains, were lost or transferred to the space during the heating season from September 1981 to March 1982 . In Table 5.11, the energy transfers or losses from the bin and the duct section between the collector and the bin were about 21.5 % of the total solar energy collected. The losses from the other components of the thermal air system were comparatively small.

Only a small percentage of solar energy was lost during the months of November, December and January. The majority of the solar energy collected was immediately used for space heating and little solar energy was stored in the storage bin. For the other months, the energy loss increased as the energy delivered to storage increased.

Table 5.12   Monthly Energy Transfers From The
            Whole Thermal Air System

Month	Yr	Monthly Collected energy Qmsun (MJ)	Monthly Heating Load Qmt (MJ)	Monthly Electric Heating Qmeh (MJ)	Monthly Solar Heating Qmas (MJ)	Monthly System Loss Qsysl (MJ)	Percent Solar Loss Łsys (%)
Sep	81	1473.0	2308.6	1631.3	677.3	795.7	54.0
Oct	81	904.4	4705.3	3927.5	777.8	126.6	14.0
Nov	81	982.3	6595.6	5691.3	904.3	78.0	7.9
Dec	81	871.0	10350.6	9533.2	817.4	53.6	6.2
Jan	82	669.3	13907.9	13264.5	643.4	25.9	3.9
Feb	82	1475.0	10823.2	9508.2	1315.0	160.0	10.8
Mar	82	2129.1	7943.3	6418.7	1524.6	604.5	28.4
Total		8415.1				1838.7	
Season							21.9

6. Conclusions And Recommendations

6.1 Conclusions

The performance characteristics and the energy flows for the air solar heating system for Module 6 at the Alberta Home Heating Research Facility have been measured for the September 1981 to March 1982 heating period. Analysis of the data gave the following conclusions.

1. The monthly solar contribution was found to be 11.8 % by the solar required method, 15.7 % by the solar supply method, 13.8 % by the building heat loss method, 11.3 % by the power records method, and 17.8 % by the F-chart method. By comparing the values 11.8 % and 15.7 % of the direct method, the most probable value of solar contribution is about 14 % during the heating season. The results indicate that:

    a. The indirect methods are acceptable methods to assess the solar contribution.

    b. Long-term monthly solar assessment by the indirect methods should be closer to the actual measured solar contribution.

2. $Fr(\tau\alpha)\epsilon$ values obtained from the collector efficiency curve were 0.53 and 0.54 on the hourly basis, 0.55 on the daily basis and 0.56 on the monthly basis. These are higher than the performance test value of 0.5.

3. The collector heat loss coefficient FrU^L was found to be 1.43 W/m²-°C and 1.58 W/m²-°C on the hourly basis,

2.56 W/m²-°C on the daily basis and 2.61 W/m²-°C on the monthly basis. These are lower than 2.9 W/m²-°C obtained from the performance test. The monthly F_rU_L value of 2.61 W/m²-°C is probably the most representative of the collector heat losses.

4. The monthly collector operating time was found to range from 60.2 hours of January 1982 to 172.8 hours of March 1982. The operation hours for each month were about the same as the monthly bright sunshine hours.

5. On a cloudless day, the collector thermal efficiency curve for the morning was found to be different from that in the afternoon. The main reasons are:

    a. The collected energy absorbed by the collector components in the morning and released in the afternoon.

    b. The rate of change in solar radiation in the morning is different from that in the afternoon.

6. On a cloudless day, the air temperature and the rock bed temperature at the top of the bin reached a maximum shortly after solar noon. As the air temperature at the collector outlet decreased in the afternoon, the top of the rock bed cooled and the maximum rock bed temperature moved to a lower level of the bin. Temperature stratification in the bin decreased and lower temperatures were available when the system changed to the heat-from-storage mode.

7. There are 3525.3 MJ of solar energy stored in the bin. A

total of 834.6 MJ which is about 23.6 % of this stored
energy, was lost from the bin. This energy loss was
great during the heating season but still acceptable.

8. For the whole thermal system, there was 8415.1 MJ of the
total solar energy collected by the collectors.
Therefore, 1838.7 MJ, which is about 21.9 % of the total
collected energy, was lost or transferred to the space.
These energy losses contributed to the heating load,
and, during September 1981, resulted in overheating the
module.

6.2 Recommendations

1. The dynamic behavior of the rock bed storage bin can be
studied in more detail by installing thermocouples at
different levels of the bin.

2. A cloudless period in August may be used to evaluate the
adequacy of the size of storage bin for the summer
period, and to study the insulation requirements to
prevent overheating of the space due to energy transfer
from storage bin and ducts.

3. The experimental dark test recommended by Edwards and
Rhee[43] can be used to correlate the instantaneous
morning and afternoon data for estimating the two
parameters of $Fr(\tau\alpha)\epsilon$ and FrU^L.

4. Simulation of solar components by existing computer
programs may be used to study the theoretical
hour-by-hour performance of the thermal air system.

References

1. ASHRAE Standard 93-77, "Methods of Testing to Determine the Thermal Performance of Solar Colectors", ANSI. B198.1-1977, The American Society of Heating, Refrigerating and Air Conditioning Engineers, New York, N.Y., 1977.

2. ASHRAE Standard 94-77, "Methods of Testing Thermal Storage Devices Based on Thermal Performance", ANSI. B199.1-1977, The American Society of Heating, Refrigerating and Air Conditioning Engineers, New York, N.Y., 1977.

3. ARI Standard 910-77, "Standard for Solar Collector", Air Conditioning and Refrigeration Institute, 1815 North Fort Myer Drive, Arlington, Virginia 22209, 1978.

4. "S.E.I.A. Certified Thermal Performance Rating Standard For Solar Collectors", S.E.I.A. Product Certification Standard 1-79, Solar Energy Industries Association, Suite 800, 1001 Connecticut Avenue, N.W., Washington D.C. 20036, Febuary 1978.

5. "Thermal Performance Rating Method for Solar Collectors", Document RMD5, SEREF., Rating Method Committee, Solar Energy Research and Education Foundation, Suite 800, 1001 Connecticut Avenue, N.W., Washington, D.C., 20036, November 14, 1978.

6. Close, D.J., "Solar Air Heaters for Low and Moderate Temperature Applications", Solar Energy, Vol. 7, pp 117, 1963.

7. Whillier, A., "Black-Painted Solar Air Heaters of Conventional Design", Solar Energy, Vol. 8, No 1, 1964.

8. Lunde, P.J., "Prediction of Average Efficiency from Climatic Data", Solar Energy, Vol. 19, pp 685-689, 1977.

9. Lunde, P.J., "Prediction of the Monthly and Annual Performance of Solar Heating Systems", Solar Energy, Vol. 20, pp 283-287, 1978.

10. Swanson, S.R., Boehm, R.F., "Calculation of Long-term Solar Collector Heating System Performance", Solar Energy, Vol. 19, pp 129-138, 1977.

11. Klein, S.A., Beckman, W.A., Duffie, J.A., "A Design Procedure for Solar Heating System", Solar Energy, Vol. 18, pp 113, 1976.

12. Klein, S.A., Cooper, P.I., Freeman, T.L., Beekman, D.M., Beckman, W.A., Duffie, J.A., "A Method of Simulation of Solar Processes and Its Application", Solar Energy, Vol. 17, pp 29-37, 1975.

13. Klein, S.A., "Calculation of Flat-plate Collector Loss Coefficients", Solar Energy, Vol. 17, pp 79-80, 1975.

14. Gupta, G.L., Garg, H.P., "Performance Studies on Solar Air Heaters", Solar Energy, Vol. 11, No. 1, pp 25, 1967.

15. Löf, G.O.G., "Air-Based Solar Systems for Space Heating", Solar Energy Handbook, Chapter 12, pp 1-34, McGraw-Hill Book Company, New York, 1981.

16. Taylor, S.L., "Assessment of Air Solar System Performance with Alternate Methods of Analysis", Solar Engineering 1981, pp 277-289, Proceedings of the ASME

Solar Energy Divison Third Annual Conference on Systems
Simulation, Economic Analysis / Solar Heating and
Cooling Operation Results, RENO,NEVADA, April 27 - May
1, 1981.

17. Löf, G.O.G., Shaw, L.E., Oank, R.L., "Comparison of
Performance of Solar Collectors of the Air Heating
Types", Presented at the 1975 International Congress,
Solar Use Now - A Resource for People, 1975.

18. Persons, R.W., Duffie, J.A., Mitchell, J.W., "Comparison
of Measured and Predicted Rock Bed Storage Performance",
Solar Energy, Vol. 24, pp 199-201, 1980.

19. Hughes, P.J., Klein, S.A., Close, D.J.,"Packed-bed
Thermal Storage Modules for Solar Air Heating and
Cooling System", J. Heat Tran., ASME 98, pp 336-337,
1976.

20. Smith, C.C., Weiss, T.A., "Design Application of the
Hottel-Whillier-Bliss Equation", Solar Energy, Vol. 19,
pp 109-113, 1977.

21. Siebers, D.L., Viskanta, R., "Comparison of Long-term
Flat Plate Solar Collector Performance Calculations
Based On Average Meteorological Data", Solar Energy,
Vol. 19, pp 163-169, 1977.

22. Hill, J.E., Streed, E.R., "A Method of Testing for
Rating Solar Collectors Based On Thermal Performance",
Solar Energy, Vol. 18, pp 421-429, 1976.

23. Hill, J.E., "Standard Procedures for Collector
Performance Testing", Solar Energy Technology Handbook,

Chapter 15, pp 457-480, Marcel Dekker, New York and Basel, 1980.

24. Gilpin, R.R., Dale, J.D., Forest, T.W., Ackerman, M.Y., "Construction of the Alberta Home Heating Research Facility and Results for the 1979-1980 Heating Season", Department of Mechanical Engineering, University of Alberta, Departmental Report No.23, August 1980.

25. Gilpin, R.R., Forest, T.W., Ackerman, M.Y., Wilson, D.J., Sadler, G.W., Dale, J.D., Zaheeruddin, M., "Second Annual Report on the Alberta Home Heating Research Facility and Results for the 1980-1981 Heating Season", Department of Mechanical Engineering, University of Alberta, Departmental Report No.24, June 1981.

26. Duffie, J.A., Beckman, W.A., *"Solar Energy Thermal Processes"*, John Wiley and Sons, New York, 1974.

27. Duffie, J.A., Beckman, W.A., *"Solar Energy of Thermal Processes"*, John Wiley and Sons, New York, 1980.

28. Kreith, F., Kreider, J.F., *"Principles of Solar Engineering"*, McGraw-Hill Book Company, New York, 1978.

29. Wijeysundera, N.W., "Response Time of Solar Collector", Solar Energy, Vol. 18, pp 65-68, 1976.

30. Beckman, W.A., Klein, S.A., Duffie, J.A., *"Solar Heating Design by the F-chart Method"*, John Wiley and Sons, New York, 1977.

31. "TRNSYS, A Transient Simulation Program", Solar Energy Laboratory, University of Wisconsin, June 1981.

32. Löf, G.O.G., Jones, D., Shaw, L.E., "A Reliable Method

for Rating Solar Collectors", Solar Engineering-1981, pp
216-225, Proceedings of the ASME Solar Energy Divison
Third Annual Conference on Systems Simulation, Economic
Analysis / Solar Heating and Cooling Operation Results,
RENO,NEVADA, April 27 - May 1, 1981.

33. Hill, J.E., Streed, E.R., "Testing and Rating of Solar
Collector", Applications of Solar Energy for Heating and
Cooling of Building, ASHRAE GRP 170, 1977.

34. Marschall, E., Adams, G., "The Efficiency of Solar
Flat-plate Collectors", Solar Energy, Vol. 20, pp
413-414, 1978.

35. Close, D.J., Yusoff, M.B., "The Effects of Air Leaks on
Solar Air Collector Behaviour", Solar Energy, Vol. 20,
pp 459-463, 1978.

36. Klein, S.A., Beckman, W.A., Duffie, J.A., "A Design
Procedure for Solar Air Heating Systems", Solar Energy,
Vol. 19, pp 509-512, 1977.

37. Kerr, R.G., Shapiro, M.M., "The Performance of a Site
Built, Air Heating, Vertical Collector With Snow
Reflector in Quebec", Solar Energy Update-78, 3-1-10, pp
1-12, 1978.

38. Kenna, J.P., "A Method of Rating Solar Collector", Solar
Energy, Vol. 29, No.5, pp 431-434, 1982.

39. Hottel, H.C., Woertz, B.B., "The Performance of
Flat-Plate Solar Heat Collectors", ASME Transactions,
Vol. 64, pp 91, 1942.

40. Bliss, R.W., "The Derivation of Several

'Plate-Efficiency Factors' Useful in Design of
Flat-plate Solar Heat Collectors", Solar Energy, Vol. 3,
No.4, pp 55, 1959.

41. Whillier, A., "Prediction of Performance of Solar
Collectors", Chapter VIII of "Applications of Solar
Energy for Heating and Cooling of Buildings", ASHRAE GRP
170, ASHRAE, New York, 1977.

42. Hollands, K.G., Chinneck, J.W., Chanarasheker, M.,
"Collector and Storage Efficiencies in Solar Heating
System", Solar Energy, Vol. 23, pp 471-478, 1980.

43. Edwards, D.K., Rhee, S.J., "Experimental Correction of
Instantaneous Collector Efficiency for Transient Heating
or Cooling", Solar Energy, Vol. 26, pp 267-270, 1981.

44. Close, D.J., "A Design Approach for Solar Processes",
Solar Energy, Vol. 11, No. 2, pp 111-122, 1967.

45. Connor, D.W., "Low-Temperature Sensible Heat Storage",
Solar Energy Technology Handbook, Chapter 23, pp
721-746, Marcel Dekker, Inc., New York and Basel, 1980.

Appendices

Appendix A-1

Table A-1 Meteorological And Thermal System Data

Day	Time Hr	Ambient Temp Ta Deg.C	Room Temp. Tr Deg.C	Air Temp. At Collector Inlet Tfi Deg.C	Air Temp At Collector Outlet Tfe Deg.C	Air Temp. At bin Top Tst Deg.C	Air Temp. At bin Bottom Tsb Deg.C	Power Usage Pow W	Electric Heating Mode EH M	DTseh Deg.C	Heat From Storage Mode HFS M	DThfs Deg.C	Heat Collection Mode COL M	DTScol Deg.C	DTCcol Deg.C	Heat From Collector Mode HFC M	DTShfc Deg.C	DTChfc Deg.C	Radiation On Tilted Surface Ht W/m2
22082	100	-4.1	20.7	13.1	3.4	35.8	21.5	2547	24	14.1	0	0.0	0	0.0	0.0	0	0.0	0.0	0.0
22082	200	-5.2	20.8	11.9	2.5	32.2	21.4	2530	22	10.6	0	0.0	0	0.0	0.0	0	0.0	0.0	0.0
22082	300	-6.2	20.8	9.3	1.7	29.8	21.4	1756	20	8.5	0	0.0	0	0.0	0.0	0	0.0	0.0	0.0
22082	400	-6.5	20.5	14.3	1.8	27.5	21.2	4926	50	6.8	0	0.0	0	0.0	0.0	0	0.0	0.0	0.0
22082	500	-6.7	20.7	12.4	1.5	25.8	21.3	3939	34	4.1	0	0.0	0	0.0	0.0	0	0.0	0.0	0.0
22082	600	-6.9	20.7	11.7	1.3	24.6	21.3	3134	26	2.9	0	0.0	0	0.0	0.0	0	0.0	0.0	0.0
22082	700	-5.2	20.7	12.1	1.9	23.7	21.2	3170	26	2.3	0	0.0	0	0.0	0.0	0	0.0	0.0	0.0
22082	800	-3.9	20.7	10.6	3.1	23.2	21.3	1889	28	1.9	0	0.0	0	0.0	0.0	0	0.0	0.0	0.0
22082	900	-1.7	20.7	18.5	12.7	22.4	21.1	4445	34	1.5	0	0.0	0	0.0	0.0	0	0.0	0.0	0.0
22082	1000	-0.4	20.1	19.5	29.0	22.9	21.3	537	0	0.0	0	0.0	4	5.5	29.6	36	1.6	16.9	679
22082	1100	-0.3	20.8	21.7	48.2	23.5	21.2	608	0	0.0	0	0.0	60	26.1	32.8	56	2.2	26.5	812
22082	1200	0.6	21.1	21.9	54.5	46.9	21.2	629	0	0.0	0	0.0	60	32.7	38.7	0	0.0	0.0	926
22082	1300	2.6	20.9	21.9	60.3	53.6	21.2	636	0	0.0	0	0.0	60	34.2	39.3	0	0.0	0.0	1039
22082	1400	4.1	21.0	22.2	61.1	55.3	21.4	635	0	0.0	0	0.0	60	32.4	35.9	0	0.0	0.0	970
22082	1500	3.6	21.3	22.8	58.4	53.8	21.8	626	0	0.0	0	0.0	60	26.2	27.2	0	0.0	0.0	847
22082	1600	3.0	21.3	24.3	51.4	48.6	22.7	631	0	0.0	0	0.0	46	17.9	17.3	0	0.0	0.0	663
22082	1700	1.5	21.1	25.9	42.9	41.6	24.4	509	0	0.0	12	15.2	0	0.0	0.0	0	0.0	0.0	385
22082	1800	-0.8	20.5	25.1	34.8	40.3	25.4	56	0	0.0	58	21.3	0	0.0	0.0	0	0.0	0.0	0.0
22082	1900	-2.9	20.5	19.6	17.3	44.5	23.2	1195	0	0.0	14	25.7	0	0.0	0.0	0	0.0	0.0	0.0
22082	2000	-4.9	20.9	12.5	8.9	46.6	22.3	679	0	0.0	16	26.9	0	0.0	0.0	0	0.0	0.0	0.0
22082	2100	-4.0	20.9	11.8	5.3	47.7	21.9	837	0	0.0	24	27.2	0	0.0	0.0	0	0.0	0.0	0.0
22082	2200	-4.3	20.8	12.9	4.1	47.8	21.6	1227	0	0.0	32	26.1	0	0.0	0.0	0	0.0	0.0	0.0
22082	2300	-3.6	20.7	14.4	3.8	46.4	21.5	1618	0	0.0	14	23.8	0	0.0	0.0	0	0.0	0.0	0.0
22082	0	-3.0	20.9	18.2	5.6	41.4	21.4	2102	32	20.0	0	0.0	0	0.0	0.0	0	0.0	0.0	0.0
22182	100	-3.9	20.8	14.8	4.6	35.3	21.5	3236	32	14.0	0	0.0	0	0.0	0.0	0	0.0	0.0	0.0
22182	200	-4.3	20.8	12.7	3.3	31.5	21.5	3213	26	10.1	0	0.0	0	0.0	0.0	0	0.0	0.0	0.0
22182	300	-4.4	20.8	12.5	2.9	28.7	21.4	3311	26	7.4	0	0.0	0	0.0	0.0	0	0.0	0.0	0.0
22182	400	-5.0	20.7	12.7	2.6	26.6	21.4	3515	28	5.3	0	0.0	0	0.0	0.0	0	0.0	0.0	0.0
22182	500	-4.8	20.7	13.2	3.0	25.0	21.3	3712	30	3.7	0	0.0	0	0.0	0.0	0	0.0	0.0	0.0
22182	600	-4.7	19.9	14.2	1.8	23.9	21.2	4321	40	2.9	0	0.0	0	0.0	0.0	0	0.0	0.0	0.0
22182	700	-4.6	20.9	9.1	3.7	22.9	21.4	2973	46	2.7	0	0.0	0	0.0	0.0	0	0.0	0.0	0.0
22182	800	-4.3	20.9	13.2	5.1	22.5	21.3	3154	26	1.4	0	0.0	0	0.0	0.0	0	0.0	0.0	0.0
22182	900	-5.0	21.3	14.7	30.2	22.4	21.0	3247	24	1.1	0	0.0	0	0.0	0.0	0	0.0	0.0	0.0
22182	1000	-5.4	20.7	19.6	49.0	30.9	20.9	3085	20	1.3	0	0.0	0	0.0	0.0	0	0.0	0.0	0.0
22182	1100	-4.9	21.1	21.7	57.0	50.3	21.1	619	0	0.0	0	0.0	28	19.0	29.8	38	1.6	17.3	773
22182	1200	-3.9	20.3	21.7	62.1	52.7	21.2	634	0	0.0	0	0.0	60	29.5	35.6	32	2.1	25.4	854
22182	1300	-3.8	21.1	22.0	62.2	56.1	21.8	637	0	0.0	0	0.0	32	33.0	40.5	28	30.3	40.5	1076
22182	1400	-3.7	21.2	22.1	58.7	54.1	22.7	631	0	0.0	0	0.0	60	35.3	40.4	0	0.0	0.0	1078
22182	1500	-3.9	21.2	22.6	51.8	49.0	24.4	640	0	0.0	0	0.0	60	32.7	36.4	0	0.0	0.0	982
22182	1600	-5.2	20.8	24.0	41.6	41.6	23.7	637	0	0.0	0	0.0	60	26.6	28.2	16	15.6	14.1	900
22182	1700	-8.4	20.8	24.0	27.5	43.9	22.5	723	0	0.0	30	19.7	34	18.7	18.0	6	16.2	10.2	713
22182	1800	-11.4	21.3	20.2	12.5	46.8	21.8	735	0	0.0	28	25.1	0	0.0	0.0	0	0.0	0.0	473
22182	1900	-12.7	20.9	15.7	3.4	47.9	21.5	1144	0	0.0	42	26.8	0	0.0	0.0	0	0.0	0.0	225
22182	2000	-13.6	20.3	9.7	2.6	48.9	21.1	979	0	0.0	36	28.3	0	0.0	0.0	0	0.0	0.0	0.0
22182	2100	-15.4	20.9	12.9	0.5	46.2	20.7	314	0	0.0	38	28.3	0	0.0	0.0	0	0.0	0.0	0.0
22182	2200	-16.2	20.3	14.5	-0.6	40.4	20.9	1988	0	0.0	2	26.6	0	0.0	0.0	0	0.0	0.0	0.0
22182	2300	-16.2	20.3	15.2	-0.6	40.4	20.7	3075	58	19.7	0	0.0	0	0.0	0.0	0	0.0	0.0	0.0
22282	0	-16.1	20.4	9.0	-1.9	33.5	20.9	2501	38	12.8	0	0.0	0	0.0	0.0	0	0.0	0.0	0.0

Ht - Solar Radiation On The Collector Tilted Surface
Only During The Collector Operation Mode On

Appendix A-2

Table A-2 UA Factors Of Module 5 And Module 6 For Some
Days With Little Or No Solar Radiation

Month Yr		Electric Power Usage		Temperature Difference of Room and Ambient		Building Heat Loss Coefficient (UA Factor)	
(ND)		P5 (kW)	P6 (kW)	DTRA5 (°C)	DTRA6 (°C)	UA5 (W/°C)	UA6 (W/°C)
Sep (0)	81	——	——	——	——	——	——
Oct (3)	81	178.1	159.4	1264.4	1240.6	140.8	128.5
Nov (7)	81	519.7	484.9	3651.7	3612.5	142.2	134.2
Dec (7)	81	664.3	652.6	4957.0	4942.9	134.0	132.0
Jan (9)	82	1037.7	1044.2	8080.6	7986.8	128.4	130.7
Feb (5)	82	519.7	500.2	3868.2	3831.1	134.3	130.6
Mar (5)	82	462.0	436.0	3426.6	3372.7	134.8	129.3
Average						135.7	130.9

ND - Number of days selected to be investigated and
with little solar radiation

From Equation 3.19

$$F_{ua} = \frac{\text{Monthly Average UA6}}{\text{Monthly Average UA5}}$$

$$= \frac{130.9}{135.7} = 0.97$$

104

Appendix A-3

UA Factor Of Module 6 Using January 1982
As The Analysis Period

Monthly Electrical Energy Usage
In January 1982   = 13264.5 MJ

Monthly Total Temperature Difference
Between The Room And Ambient   = 28256 °C
Temperature In January 1982

From Equation 3.18

$$UA = \frac{13264.5}{28256.0} \times \frac{1 \times 10^6}{3600}$$

$$= 130.4 \text{ W/°C}$$

Appendix A-4

Conversion Of The Test Performance

Collector Area = 19.5 ft² = 1.81 m²

Air Flow Rate = 2 CFM/ft²
= 0.0102 m³/s-m²
= 0.0184 m³/s

The original parameters of the test performance :

$F_o U^L$ = 0.67 BTU/ft²-h-°F = 3.8 W/m²-°C
$F_o(\tau\alpha)_n$ = 0.65

Cp = 1006 J/kg-°C

ρ = 1.204 kg/m³

$\left.\begin{array}{c} \\ \\ \end{array}\right\}$ at 70 °F
$\cong$ 21 °C

From reference of Beckman and Duffie[26]

$$\frac{\bar{m}Cp}{Ac} = \frac{1.204(0.0184)1006}{1.8} = 12.38 \text{ W/m}^2\text{-}°C$$

The Standard parameters become :

$$FrU^L = F_o U^L \left[\frac{\dfrac{\bar{m}Cp}{Ac}}{\dfrac{\bar{m}Cp}{Ac} + F_o U^L} \right]$$

$$= 3.8 \left[\frac{12.38}{12.38 + 3.8} \right] = 2.9 \text{ W/m}^2\text{-}°C$$

$$Fr(\tau\alpha)_n = F_o(\tau\alpha)_n \left[\frac{\dfrac{\bar{m}Cp}{Ac}}{\dfrac{\bar{m}Cp}{Ac} + F_o U^L} \right]$$

$$= 0.65 \left[\frac{12.38}{12.38 + 3.8} \right] = 0.5$$

B30364